Electronic Supplementary Material (ESI) for ChemComm.

Supporting Information

Reversible dehydrogenation of a primary aryl borane

*Connor S. MacNeil, Shou-Jen Hsiang, and Paul G. Hayes**

Department of Chemistry and Biochemistry
Canadian Centre for Research in Advanced Fluorine Technologies
University of Lethbridge, Lethbridge, Alberta, Canada T1K 3M4

p.hayes@uleth.ca

Table of Contents

General Considerations	S2
Preparation of Organoboranes and Rhodium Complexes	S4
NMR Spectra	S12
Crystallographic Details	S33
Computational Details	S38
References	S49

I. General Considerations

All air- and moisture-sensitive manipulations were carried out using vacuum line, Schlenk and cannula techniques, or in an MBraun inert atmosphere (argon) glove box unless otherwise noted. All glassware was stored in a pre-heated (110 ºC) oven or flame-dried prior to use. Solvents used for air-sensitive procedures were purified using an MBraun solvent purification system (SPS), stored in PTFE-sealed glass vessels over sodium benzophenone ketyl (THF, pentane, benzene, and toluene), and distilled at the time of use. Benzene-d_6 was dried over sodium benzophenone ketyl, distilled *in vacuo* and stored over 4 Å molecular sieves in PTFE-sealed glass vessels under argon.[1] Aryldihydroboranes H_2BMes and H_2BAr^F, and **1-CO** were prepared according to literature procedures.[2,3] Pinacol, $B(OMe)_3$, 2-bromomesitylene, and $BH_3{\cdot}SMe_2$ were purchased from Sigma-Aldrich and used without further purification. 1,3-bis(trifluoromethyl)-5-bromobenzene was purchased from Alfa Aesar and used as received. Unless otherwise noted all NMR spectra were recorded at ambient temperature with a Bruker Avance II NMR spectrometer (300.13 MHz for ^{1}H, 96.29 MHz for ^{11}B, 75.47 MHz for ^{13}C, 282.40 MHz for ^{19}F and 121.48 MHz for ^{31}P) or Avance III NMR spectrometer (700.44 MHz for ^{1}H, 224.63 MHz for ^{11}B, 176.13 MHz for ^{13}C, 658.78 MHz for ^{19}F and 283.54 MHz for ^{31}P) NMR spectrometer. All ^{1}H and ^{13}C NMR chemical shifts are reported in ppm relative to $SiMe_4$ using the ^{1}H (benzene-d_6: 7.16 ppm) and ^{13}C (benzene-d_6: 128.06 ppm) chemical shifts of the solvent as a standard.[4] ^{11}B NMR chemical shifts were referenced externally to $BF_3{\cdot}Et_2O$ (δ 0.0). ^{19}F NMR chemical shifts were referenced externally to C_6H_5F (δ –113.11 in benzene-d_6).[5] ^{31}P NMR chemical shifts were reference to external 85% H_3PO_4 in H_2O (δ 0.0). ^{1}H NMR data for diamagnetic compounds are reported as follows: chemical

shift, multiplicity (s = singlet, d = doublet, t = triplet, q = quartet, quint = quintet, sp = septet, br = broad, m = multiplet, app = apparent, obsc = obscured, ov = overlapping), coupling constants (Hz), integration, assignment. ^{13}C NMR data for diamagnetic compounds are reported as follows: chemical shift, assignment. Assignment of resonances were supplemented by $^{1}H–^{1}H$ COSY, $^{13}C\{^{1}H\}$ APT, $^{1}H–^{13}C\{^{1}H\}$, and HSQC/HMBC experiments.

Elemental analyses (%CHN) were conducted at the University of Lethbridge on an Elementar Americas Vario MicroCube Analyzer (C, H, N, O, S capabilities) using bulk recrystallized compounds. Infrared spectroscopy was conducted on a Thermo-Nicolet iS10 FT-IR spectrometer using bulk recrystallized compounds.

II. Preparation of Organoboranes and Rhodium Complexes

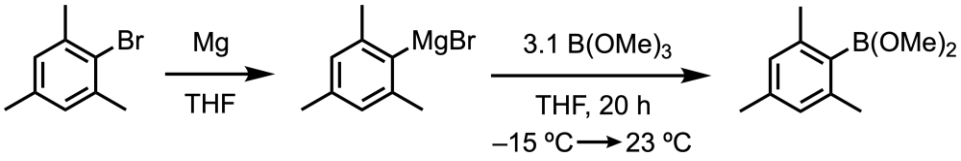

$(OMe)_2BMes$. Adapting from a literature procedure,[2a] an oven-dried 250 mL 3-neck round-bottomed flask was charged with a stir bar, 2.803 g of magnesium turnings, and a small crystal of iodine (I_2). The flask was evacuated on a double-manifold vacuum line and cooled to –78 ºC. Approximately 15 mL of THF was transferred under reduced pressure onto the magnesium turnings. A separate flask was charged with 18.2 g (91.3 mmol) of mesityl bromide which was degassed by three freeze–pump–thaw cycles. THF (70 mL) was added under reduced pressure. The THF solution was transferred *via* cannula into a 100 mL dropping funnel attached to the 250 mL flask containing the magnesium turnings. The mesityl bromide solution was added dropwise over 45 minutes, resulting in gentle bubbling and warming of the mixture. The dropping funnel was removed, and the reaction mixture was heated to reflux for 18 hours, at which point the solution was grey and opaque. The Grignard reagent was transferred *via* syringe to a 250 mL 2-neck round-bottomed flask containing 3.1 equivalents (283 mmol, 0.035 L) of $B(OMe)_3$ dissolved in 15 mL of cold (–15 ºC) diethylether. The reaction mixture became cloudy with a dense white precipitate that formed after several minutes. The mixture was warmed to ambient temperature, stirred for 20 hours and then diluted with 150 mL of pentane. The supernatant was transferred *via* cannula into a 500 mL Teflon-sealed thick-walled flask. Volatiles were removed under reduced pressure to afford

dimethoxymesitylborane as a colorless oil (10.5 g, 60% yield). NMR data (^{1}H, ^{11}B) agreed well with literature data.[2]

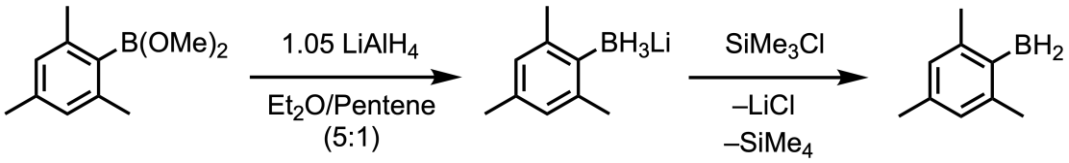

H_2BMes. A 100 mL round-bottomed flask was charged with a stir bar and 2.00 g (0.010 mol) of freshly distilled $(OMe)_2$BMes dissolved in 60 mL of a 5:1 mixture of diethylether and pentane. The mixture was then cooled to 0 ºC. In a separate 50 mL round-bottomed flask 1.05 equivalents of $LiAlH_4$ (0.415 g) was suspended in diethylether (20 mL). The $LiAlH_4$ slurry was added dropwise to the cold (0 ºC) stirring $(OMe)_2$BMes solution over 2 minutes. The mixture was allowed to gradually warm to ambient temperature whereupon it was stirred for 3 hours. The product was filtered through a pad of Celite and washed with a 1:1 mixture of pentane and diethylether (3 x 5 mL). Volatiles were removed under reduced pressure to afford Li[H_3BMes] as a white solid (0.408 g, 28% yield). NMR data (^{1}H, ^{11}B) agreed well with literature data.[2] One equivalent of Me_3SiCl (0.232 g, 0.002 mol) was added to a diethylether solution of Li[H_3BMes] (0.302 g, 0.002 mol) at ambient temperature. The reaction mixture was rapidly stirred for 3 hours during which a white precipitate formed. The solvent was removed under vacuum and the residue extracted with pentane (3 x 5 mL) to yield H_2BMes as a crystalline white solid (0.358 g, 95% yield from Li[H_3BMes]). NMR data (^{1}H, ^{11}B) agreed well with literature data.[2] Note: It is not necessary to isolate Li[H_3BMes]. It can be generated and used *in situ*.

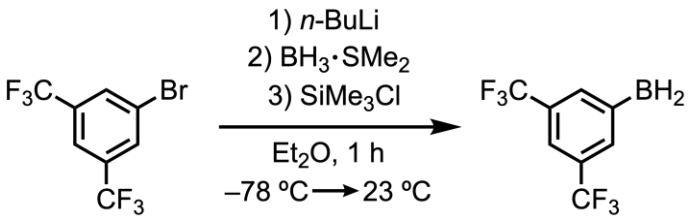

H_2BAr^F. Following a literature procedure,[2b] 150 mL Teflon-sealed thick-walled flask was charged with 3,5-bis(trifluoromethyl)bromobenzene (1.07 g, 3.62 mmol) and 20 mL of diethylether. The solution was degassed by three freeze–pump–thaw cycles and cooled to –78 ºC. Under an atmosphere of argon, 1.45 mL (1 equivalent, 3.62 mmol) of *n*-butyl lithium (2.5 M in hexanes) was added dropwise *via* syringe over 10 minutes. The solution turned from colorless to yellow during 15 minutes of stirring. The mixture was quenched with 0.343 mL of BH_3•SMe_2 (1 equivalent, 3.62 mmol), added over 30 seconds *via* syringe. The reaction mixture was warmed to 23 ºC, becoming a pale-yellow color. After 1 hour at 23 ºC, Me_3SiCl (0.46 mL, 1 equivalent, 3.6 mmol) was added *via* syringe over 10 seconds, yielding H_2BAr^F as a pale-orange solution. Since the product decomposes upon removal of the solvent, H_2BAr^F was used as a diethylether solution of known concentration (*e.g.* 0.287 mol L^{-1}). ^{1}H NMR (300.13 MHz, benzene-d_6): δ 8.01 (s, 2H, *m*-Ar *H*); 7.83 (s, 1H, *o*-Ar *H*); 2.85 (br s, 2H, BH_2). ^{11}B NMR (96.29 MHz, benzene-d_6): δ –9.6 (br s). ^{19}F NMR (282.23 MHz, benzene-d_6): δ –62.3 (s, 6F). NMR data (^{1}H, ^{11}B, ^{19}F) agreed well with literature data.[2b]

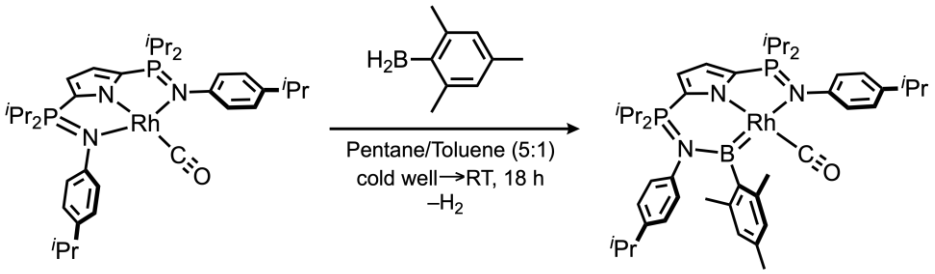

1-CO **1-BMes**

($^{i\mathrm{Pr}}$NNN)(CO)Rh=B(2,4,6-$(CH_3)_3C_6H_2$) (1-BMes). A 20 mL scintillation vial was charged with **1-CO** (0.045 g, 0.065 mmol), 1 equivalent of mesitylborane (9.1 mg, 0.066 mmol), and a Teflon-coated stir bar. The solids were dissolved in a mixture of pentane and toluene (5 mL, 5:1) giving a red-orange solution and the vial was placed in a cold well cooled with liquid nitrogen. The reaction mixture was rapidly stirred at low temperature for 1 h in the glove box with periodic sparging of the solution. The reaction solution became light-orange and was allowed to stand in the cold well for 18 h producing a dark-yellow crystalline solid. The solid was washed with cold pentane (3 x 5 mL) to yield 0.028 g (53% yield) of **1-BMes** as a bright yellow powder. Anal. Calcd. for $C_{44}H_{63}BN_3OP_2Rh$: C, 64.01; H, 7.69; N, 5.09. Found: C, 63.83; H, 7.96; N, 4.65. IR: (ν_{CO}) 1909 cm^{-1}. ^{1}H NMR (700.13 MHz, benzene-d_6): δ 7.51 (d, $^3J_{HH}$ = 7.7 Hz, 2H, 4-^{i}Pr-C$_6$*H*$_4$); 7.06 (d, $^3J_{HH}$ = 7.9 Hz, 2H, 4-^{i}Pr-C$_6$*H*$_4$); 6.93 (d, $^3J_{HH}$ = 7.7 Hz, 2H, 4-^{i}Pr-C$_6$*H*$_4$); 6.67 (d, $^3J_{HH}$ = 7.9 Hz, 2H, 4-^{i}Pr-C$_6$*H*$_4$); 6.66 (app t, $^3J_{HP}$ = $^3J_{HH}$ = 3.9 Hz, 1H, 3,4-pyrrole); 6.61 (s, 2H, Mes Ar *H*); 6.51 (dd, $^3J_{HP}$ = $^3J_{HH}$ = 3.9 Hz, 1H, 3,4-pyrrole); 3.26 (sp, $^3J_{HH}$ = 7.2 Hz, 2H, PC*H*(CH$_3$)$_2$); 2.73 (sp, $^3J_{HH}$ = 6.9 Hz, 1H, C*H*(CH$_3$)$_2$); 2.72 (s, 6H, Mes C*H*$_3$); 2.43 (sp, $^3J_{HH}$ = 6.9 Hz, 1H, C*H*(CH$_3$)$_2$); 2.19 (ov m, 2H, PC*H*(CH$_3$)$_2$); 2.09 (s, 3H, Mes C*H*$_3$); 1.16 (d, $^3J_{HH}$ = 6.9 Hz, 6H, CH(C*H*$_3$)$_2$); 1.11 (dd, $^3J_{HP}$ = 15.4 Hz, J_{HH} = 7.2 Hz, 6H, PCH(C*H*$_3$)$_2$); 1.04 (dd, $^3J_{HP}$ = 15.7 Hz, J_{HH} = 7.2 Hz, 6H, PCH(C*H*$_3$)$_2$); 0.97 (dd, $^3J_{HP}$ = 16.7 Hz, J_{HH} = 7.2 Hz, 6H, PCH(C*H*$_3$)$_2$); 0.92 (d, $^3J_{HH}$ = 6.9 Hz, 6H, CH(C*H*$_3$)$_2$); 0.85 (dd, $^3J_{HP}$ = 16.2 Hz, J_{HH} = 7.2

Hz, 6H, PCH(CH_3)$_2$). ^{11}B NMR (224.63 MHz, benzene-d_6): δ 32.6 (br s, 1B). ^{13}C{^{1}H} NMR (75.46 MHz, benzene-d_6): δ 196.6 (d, $^1J_{CRh}$ = 87.6 Hz, Rh–*C*O); 152.6 (br s, *ipso*-Mes *C*) 151.3 (s, *para*-Pipp *C*); 147.1 (s, *para*-Pipp *C*); 140.2 (d, $^2J_{CRh}$ = 2.4 Hz, *ipso*-Pipp *C*); 140.1 (m, $^2J_{CRh}$ = 3.4 Hz, *ipso*-Pipp *C*); 137.7 (dd, $^1J_{CP}$ = 145 Hz, $^3J_{CP}$ = 16.1 Hz, 2,5-pyrrole *C*); 133.6 (s, *ipso*-Mes *C*); 133.2 (s, *ipso*-Mes *C*); 129.1 (s, Ar *C*H); 127.1 (s, Ar *C*H); 126.6 (m, $^3J_{CRh}$ = 8.9 Hz, Pipp *C*H); 126.5 (s, Ar *C*H); 125.9 (s, Ar *C*H); 120.7 (ddd, $^1J_{CP}$ = 129 Hz, $^3J_{CP}$ = 13.5 Hz, $^3J_{CRh}$ = 3.4 Hz, 2,5-pyrrole *C*); 118.2 (dd, $^2J_{CP}$ = 24.6 Hz, $^3J_{CP}$ = 10.9 Hz, 3,4-pyrrole *C*H); 115.1 (dd, $^2J_{CP}$ = 24.8 Hz, $^3J_{CP}$ = 9.9 Hz, 3,4-pyrrole *C*H); 33.7 (s, *C*H(CH$_3$)$_2$); 33.6 (s, *C*H(CH$_3$)$_2$); 27.3 (s, CH(*C*H$_3$)$_2$); 26.6 (s, *C*H(CH$_3$)$_2$); 26.5 (s, *C*H(CH$_3$)$_2$); 24.1 (d, $^1J_{CP}$ = 54.9 Hz, P*C*H(CH$_3$)$_2$); 23.9 (s, 2,6-*C*H$_3$ Mes); 21.3 (s, 4-*C*H$_3$ Mes); 16.7 (m, CH(*C*H$_3$)$_2$); 16.6 (m, CH(*C*H$_3$)$_2$); 16.5 (m, CH(*C*H$_3$)$_2$); 16.4 (m, CH(*C*H$_3$)$_2$). ^{31}P{^{1}H} NMR (283.42 MHz, benzene-d_6): δ 52.6 (d, $^2J_{PRh}$ = 7.3 Hz, 1P, *P*–N–Rh); 37.8 (s, 1P, *P*–N–B).

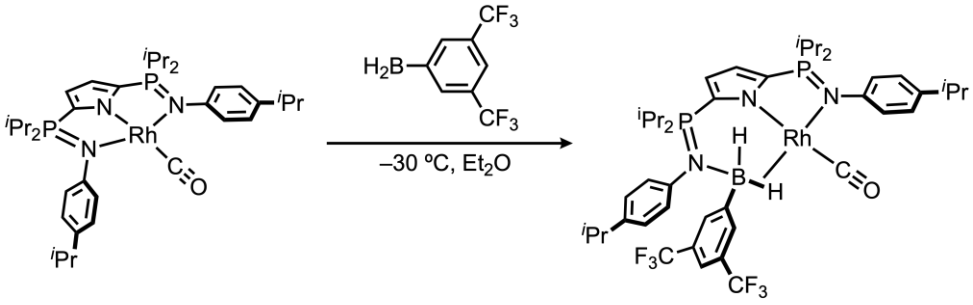

1-CO **1-CO·H_2BMes**

(*i*^{Pr}NNN)Rh(CO)H_2B(3,5-(CF$_3$)$_2$C$_6$H$_3$) (1-CO·H_2BAr^F). In a 20 mL scintillation vial, crystalline **1-CO** (0.025 g, 35.9 mmol) was dissolved in 5 mL of Et$_2$O and chilled to –30 ° C. A solution of H_2B(3,5-(CF$_3$)$_2$C$_6$H$_3$) in Et$_2$O (0.125 mL, 37 mmol) was added *via* syringe over 10 seconds. The solution was stirred at –30 °C for 2 hours becoming dark yellow in

colour. The compound was dried under vacuum and washed with pentane (2 x 3 mL) giving 0.028 g of **1-CO-H$_2$BAr^F** as a bright yellow powder (84% yield). Anal. Calcd. for $C_{44}H_{60}BF_6N_3OP_2Rh$: C, 56.04; H, 6.23; N, 4.56. Found: C, 56.16; H, 6.16; N, 4.33. IR: (ν_{CO}) 1950 cm^{-1}. ^{1}H NMR (700.13 MHz, benzene-d_6): δ 8.04 (s, 2H, *o*-Ar^F *H*); 7.68 (s, 1H, *p*-Ar^F *H*); 7.29 (d, $^3J_{HH}$ = 7.9 Hz, 2H, 4-^{i}Pr-C$_6$*H*$_4$); 7.21 (d, $^3J_{HH}$ = 7.9 Hz, 2H, 4-^{i}Pr-C$_6$*H*$_4$); 7.05 (d, $^3J_{HH}$ = 8.2 Hz, 2H, 4-^{i}Pr-C$_6$*H*$_4$); 6.83 (d, $^3J_{HH}$ = 8.2 Hz, 2H, 4-^{i}Pr-C$_6$*H*$_4$); 6.47 (app t, $^3J_{HP}$ = $^3J_{HH}$ = 3.3 Hz, 1H, 3,4-pyrrole); 6.39 (ov dd, $^3J_{HP}$ = $^3J_{HH}$ = 3.3 Hz, 1H, 3,4-pyrrole); 2.70 (sp, $^3J_{HH}$ = 6.9 Hz, 1H, C*H*(CH$_3$)$_2$); 2.60 (sp, $^3J_{HH}$ = 6.9 Hz, 1H, C*H*(CH$_3$)$_2$); 2.23 (m, 2H, PC*H*(CH$_3$)$_2$); 2.03 (m, 2H, PC*H*(CH$_3$)$_2$); 1.13 (d, $^3J_{HH}$ = 6.9 Hz, 6H, CH(C*H*$_3$)$_2$); 1.06 (d, $^3J_{HH}$ = 6.9 Hz, 6H, CH(C*H*$_3$)$_2$); 0.99 (dd, $^2J_{HP}$ = 15.5 Hz, $^3J_{HH}$ = 7.1 Hz, 6H, PCH(C*H*$_3$)$_2$); 0.90 (ov m, 12H, PCH(C*H*$_3$)$_2$); 0.84 (dd, $^2J_{HP}$ = 15.5 Hz, $^3J_{HH}$ = 7.1 Hz, 6H, PCH(C*H*$_3$)$_2$); –3.10 (br s, 2H, B*H*). ^{11}B NMR (224.63 MHz, benzene-d_6): δ –5.9 (s, 1B). ^{13}C{^{1}H} NMR (176 MHz, benzene-d_6): δ 190.6 (d, $^1J_{CRh}$ = 75.7 Hz, Rh–*C*O); 151.0 (s, Ar *C*); 146.9 (s, Ar *C*); 143.4 (s, Ar *C*); 142.9 (s, Ar *C*); 134.6 (br m, 2,5-pyrrole *C*); 129.9 (d, $^3J_{CF}$ = 4.0 Hz, Ar *C*H); 129.6 (d, $^2J_{CF}$ = 31.7 Hz, Ar *C*); 127.7 (s, Ar *C*H); 127.5 (s, Ar *C*H); 127.2 (s, Ar *C*H); 127.1 (d, $^3J_{CF}$ = 7.0 Hz, Ar *C*H); 126.6 (s, Ar *C*H); 124.6 (m, 2,5-pyrrole *C*); 118.4 (dd, $^2J_{CP}$ = 23.0 Hz, $^3J_{CP}$ = 10.4 Hz, 3,4-pyrrole *C*H); 115.2 (dd, $^2J_{CP}$ = 24.6 Hz, $^3J_{CP}$ = 11.2 Hz, 3,4-pyrrole *C*H); 33.9 (s, *C*H(CH$_3$)$_2$); 33.7 (s, *C*H(CH$_3$)$_2$); 26.8 (d, $^1J_{CP}$ = 52.8 Hz, PCH(CH$_3$)$_2$); 26.3 (d, $^1J_{CP}$ = 62.0 Hz, P*C*H(CH$_3$)$_2$); 24.3 (s, CH(*C*H$_3$)$_2$); 24.1 (s, CH(*C*H$_3$)$_2$); 17.0 (d, $^2J_{CP}$ = 2.7 Hz, PCH(*C*H$_3$)$_2$); 16.4 (d, $^2J_{CP}$ = 2.4 Hz, PCH(*C*H$_3$)$_2$); 16.2 (d, $^2J_{CP}$ = 2.7 Hz, PCH(*C*H$_3$)$_2$); 16.1 (d, $^2J_{CP}$ = 1.9 Hz, PCH(*C*H$_3$)$_2$); *ipso*-Ar^F *C* and *C*F$_3$ signals could not be located. ^{19}F{^{1}H} NMR (282 MHz, benzene-d_6): δ –62.1 (s, 6F, C*F*$_3$). ^{31}P{^{1}H} NMR (283.42 MHz, benzene-d_6): δ 51.3 (s, 1P, *P*–N–Rh); 48.8 (s, 1P, *P*–N–B).

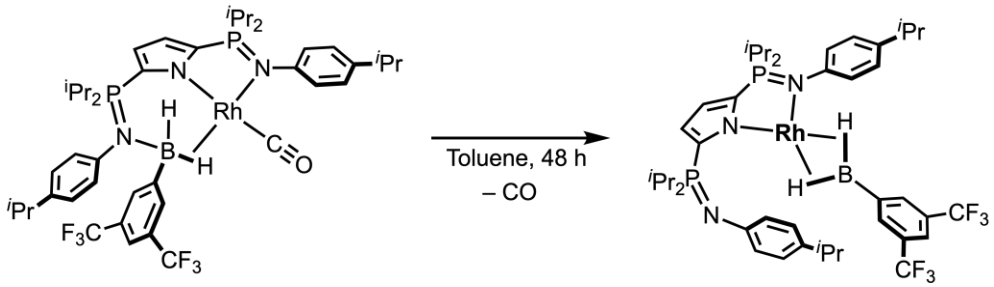

1-CO·H$_2$BAr^F **1-H$_2$BAr^F**

(*i*^{Pr}NNN)RhH$_2$B(3,5-(CF$_3$)$_2$C$_6$H$_3$) (1-H$_2$BAr^F). In a 20 mL scintillation vial, crystalline **1-CO·H$_2$BAr^F** (0.020 g, 0.022 mmol) was dissolved in 4 mL of toluene and stirred at 23 ºC for 48 h. The solvent was removed under vacuum and the product was extracted with 2 x 3 mL of pentane. The resulting solution was filtered through Celite and dried under reduced pressure to afford 0.010 g (51% yield) of **1-BAr^F** as a dark brown solid. Anal. Calcd. for $C_{42}H_{57}BF_6N_3P_2Rh$: C, 56.45; H, 6.43; N, 4.70. Found: C, 55.88; H, 6.21; N, 4.41. ^{1}H NMR (700.13 MHz, benzene-*d*$_6$): δ 7.79 (s, 2H, *o*-Ar^F *H*); 7.68 (s, 1H, *p*-Ar^F *H*); 7.33 (br s, 1H, 3,4-pyrrole); 7.13 (obsc m, 4H, 4-*i*Pr-C$_6$*H*$_4$); 6.89 (ov m, 4H, 4-*i*Pr-C$_6$*H*$_4$); 6.32 (br s, 1H, 3,4-pyrrole); 4.69 (br s, 2H, B*H*$_2$); 2.83 (m, 1H, C*H*(CH$_3$)$_2$); 2.59 (m, 1H, C*H*(CH$_3$)$_2$); 2.37 (m, 1H, PC*H*(CH$_3$)$_2$); 1.81 (m, 1H, PC*H*(CH$_3$)$_2$); 1.72 (m, 1H, PC*H*(CH$_3$)$_2$); 1.55 (br m, 1H, PC*H*(CH$_3$)$_2$); 1.40-0.40 (ov m, 36H, CH(C*H*$_3$)$_2$). ^{11}B NMR (224.63 MHz, benzene-*d*$_6$): δ 1.7 (br s, 1B). ^{13}C{^{1}H} NMR (176 MHz, benzene-*d*$_6$, 23 ºC): δ 162.0 (s, Ar *C*); 145.1 (s, Ar *C*); 143.5 (s, Ar *C*); 142.4 (s, Ar *C*); 133.7 (br m, 2,5-pyrrole *C*); 130.0 (s, Ar *C*); 129.4 (s, Ar *C*H) 127.7 (s, Ar *C*H); 127.5 (s, Ar *C*H); 126.7 (br m, Ar *C*H); 125.7 (br m, Ar *C*H); 124.7 (br m, 2,5-pyrrole *C*); 124.3 (s, Ar *C*H); 123.3 (dd, $^2J_{CP}$ = 44.9 Hz, $^3J_{CP}$ = 14.3 Hz, 3,4-pyrrole *C*H); 117.7 (dd, $^2J_{CP}$ = 36.1 Hz, $^3J_{CP}$ = 14.1 Hz, 3,4-pyrrole *C*H); 33.9 (s, *C*H(CH$_3$)$_2$); 33.7 (s, *C*H(CH$_3$)$_2$); 27.2 (d, $^1J_{CP}$ = 53.6 Hz, P*C*H(CH$_3$)$_2$); 24.8 (br m, P*C*H(CH$_3$)$_2$); 24.1 (s, CH(*C*H$_3$)$_2$); 24.0 (s, CH(*C*H$_3$)$_2$); 16.4 (br s, PCH(*C*H$_3$)$_2$); 16.3 (br s,

PCH(CH_3)$_2$); 15.9 (m, PCH(CH_3)$_2$); 15.3 (m, PCH(CH_3)$_2$); *ipso*-Ar^F and CF_3 signals could not be located. $^{19}F\{^1H\}$ NMR (282.40 MHz, benzene-d_6): δ –62.3 (s, 6F, CF_3). $^{31}P\{^1H\}$ NMR (283.42 MHz, benzene-d_6): δ 51.7 (br s, 1P, *P*–N–Rh); 11.4 (br, 1P, *P*–N).

III. NMR Spectra

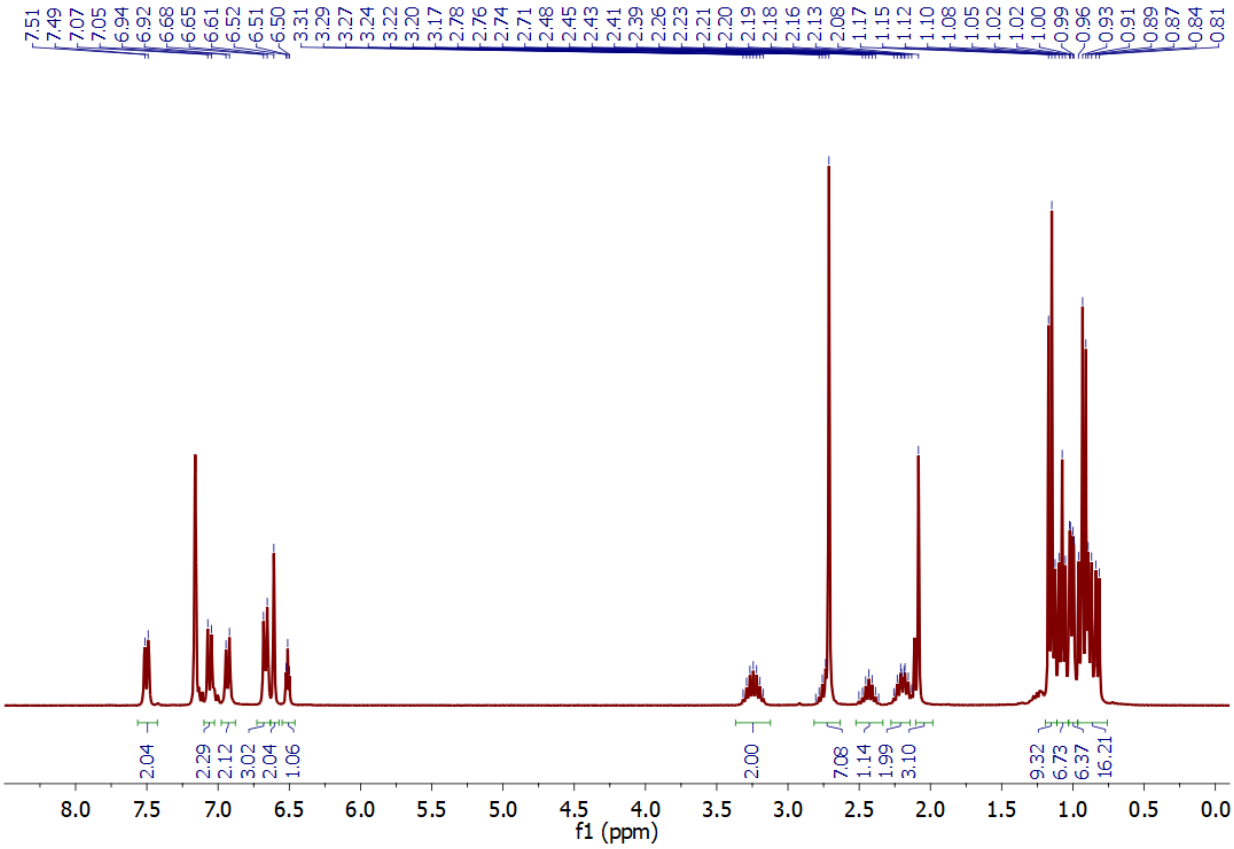

Figure S1. ^{1}H NMR (300 MHz) spectrum of **1-BMes** in benzene-d_6 at 23 ºC.

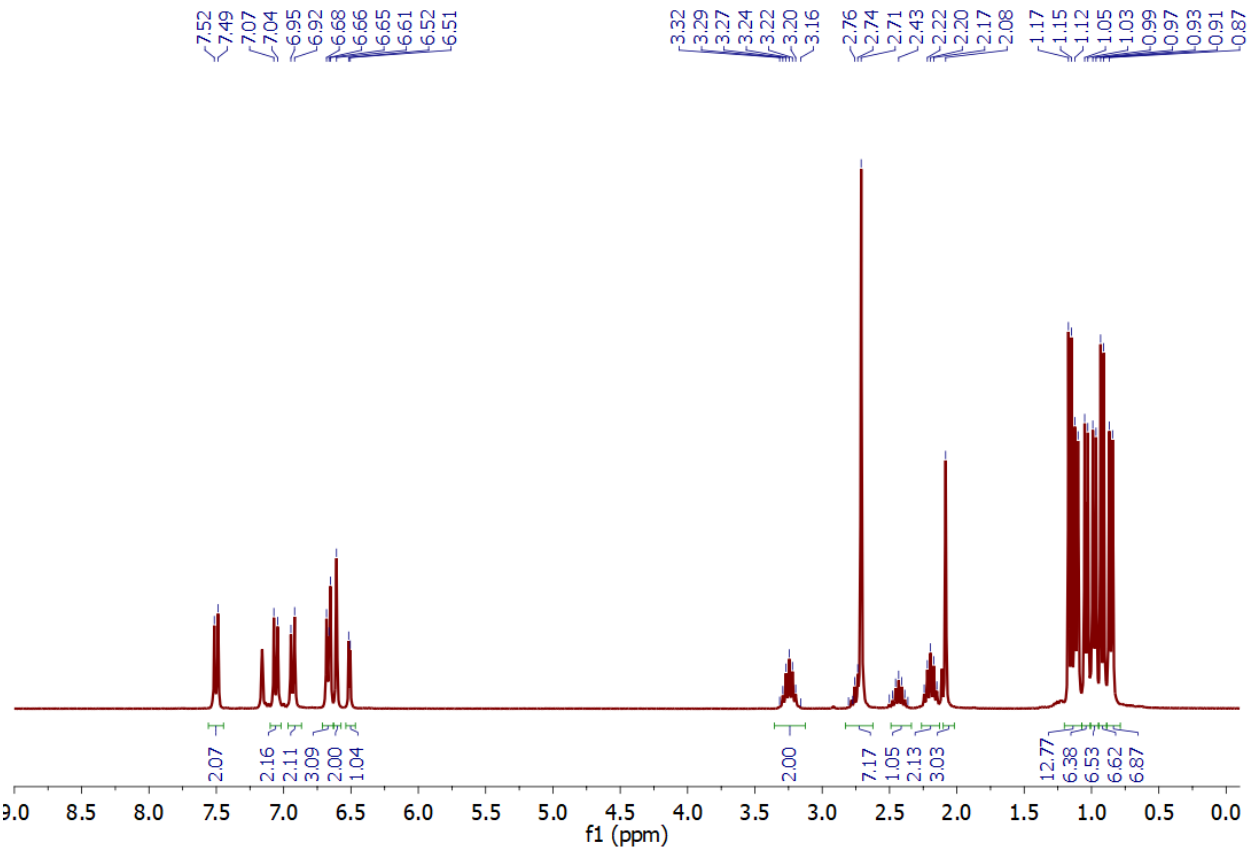

Figure S2. $^{1}H\{^{31}P\}$ NMR (300 MHz) spectrum of **1-BMes** in benzene-d_6 at 23 ºC.

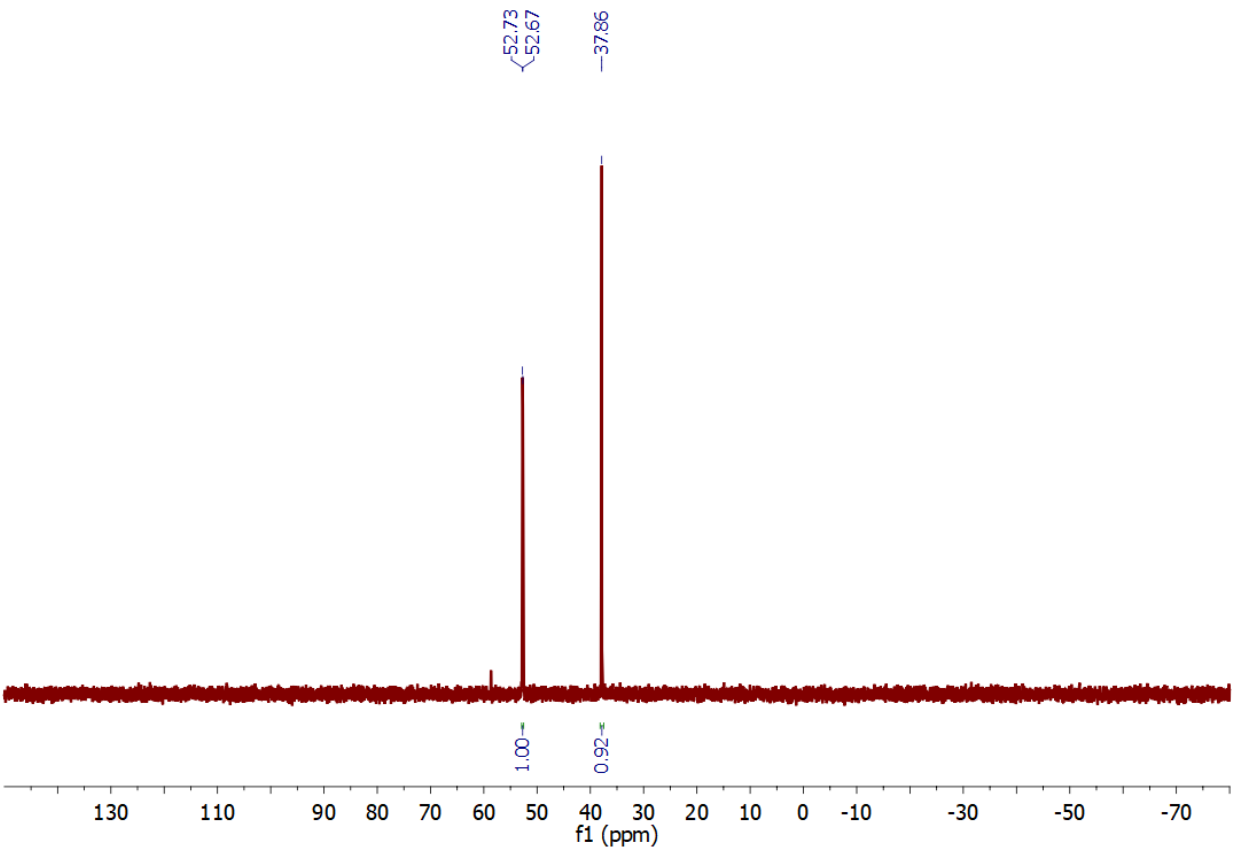

Figure S3. $^{31}P\{^{1}H\}$ NMR (121 MHz) spectrum of **1-BMes** in benzene-d_6 at 23 ºC.

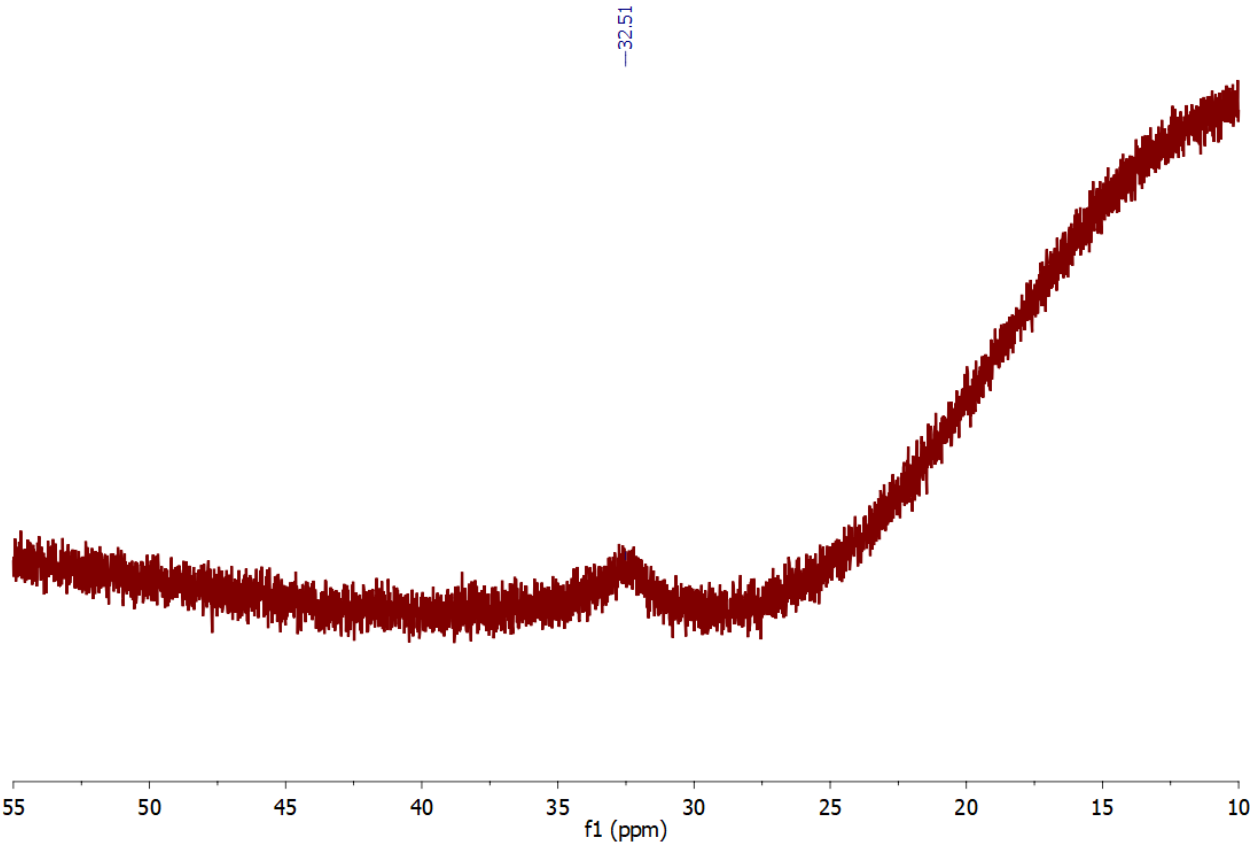

Figure S4. $^{11}B\{^{1}H\}$ NMR (224 MHz) of **1-BMes** in benzene-d_6 at 23 ºC.

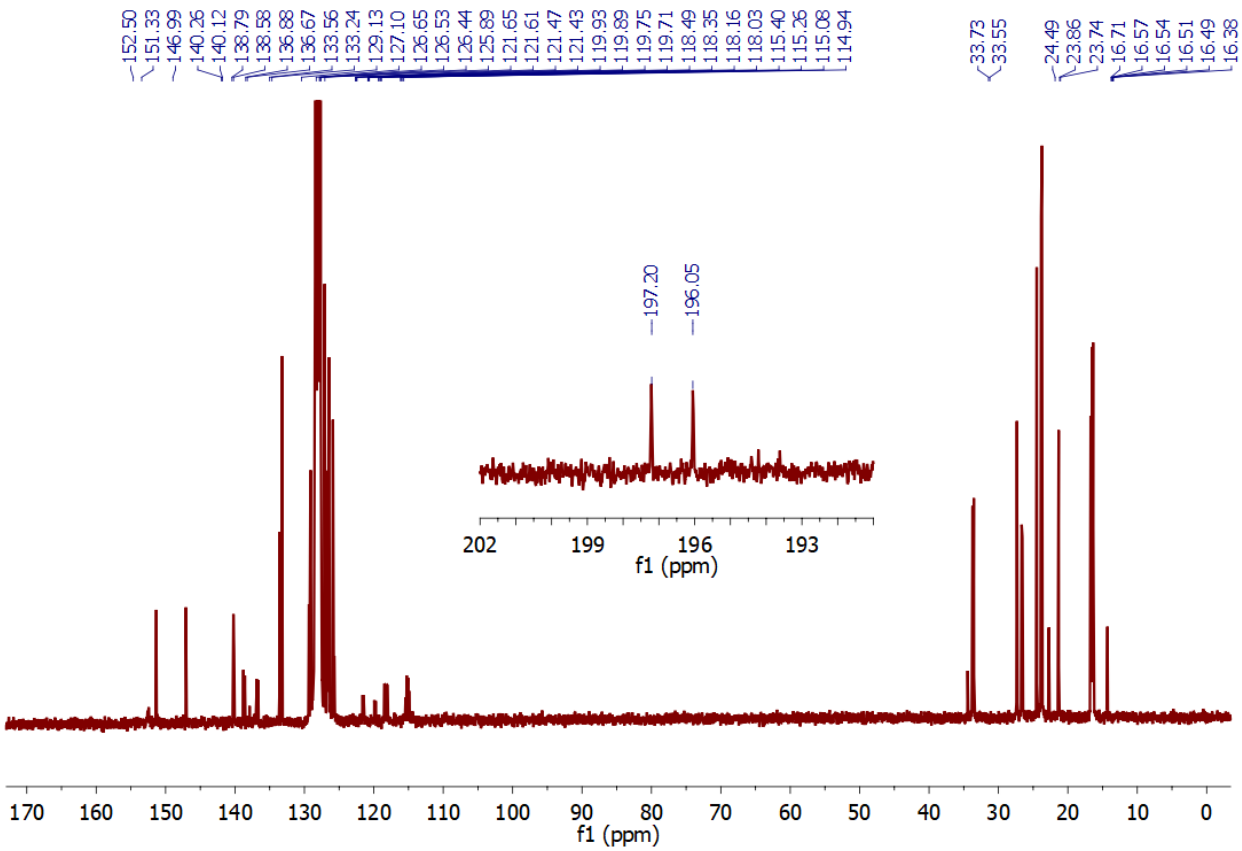

Figure S5. $^{13}C\{^{1}H\}$ NMR (75 MHz) spectrum of **1-BMes** in benzene-d_6 at 23 ºC. Inset: Rh–*C*O resonance.

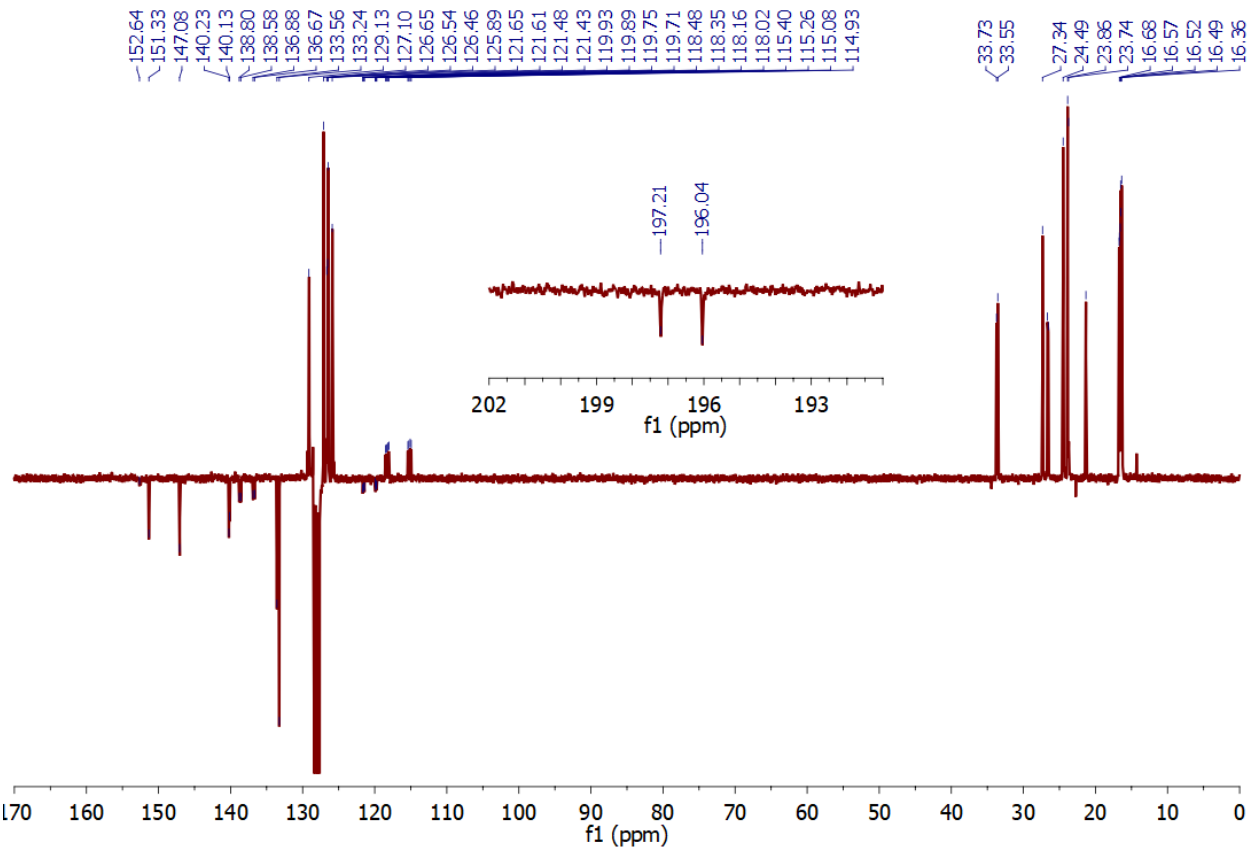

Figure S6. $^{13}C\{^{1}H\}$ APT (75 MHz) spectrum of **1-BMes** in benzene-d_6 at 23 ºC; quaternary and methylene ^{13}C phased down, methyl and methine ^{13}C phased up. Inset: Rh–*C*O resonance.

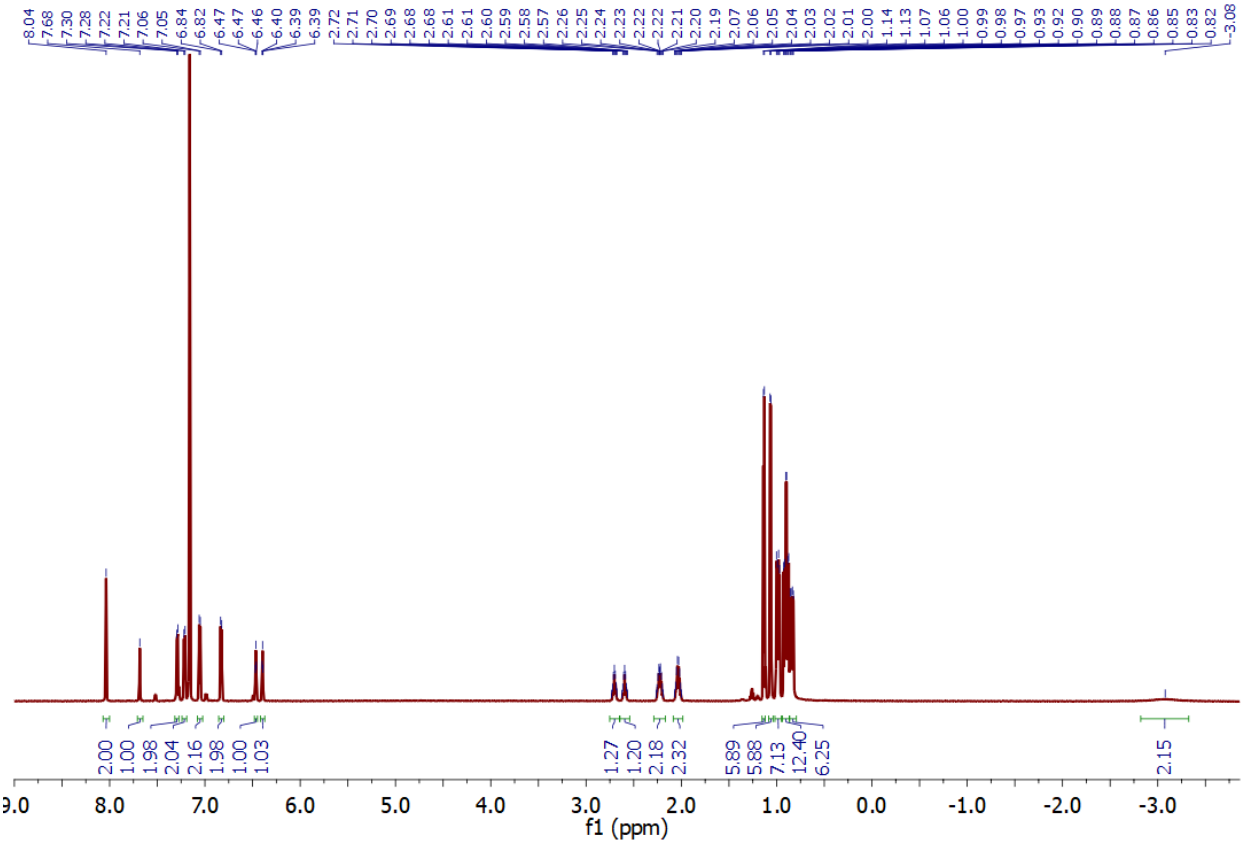

Figure S7. ^{1}H NMR (700 MHz) spectrum of **1-CO·H_2BAr^F** in benzene-d_6 at 23 ºC.

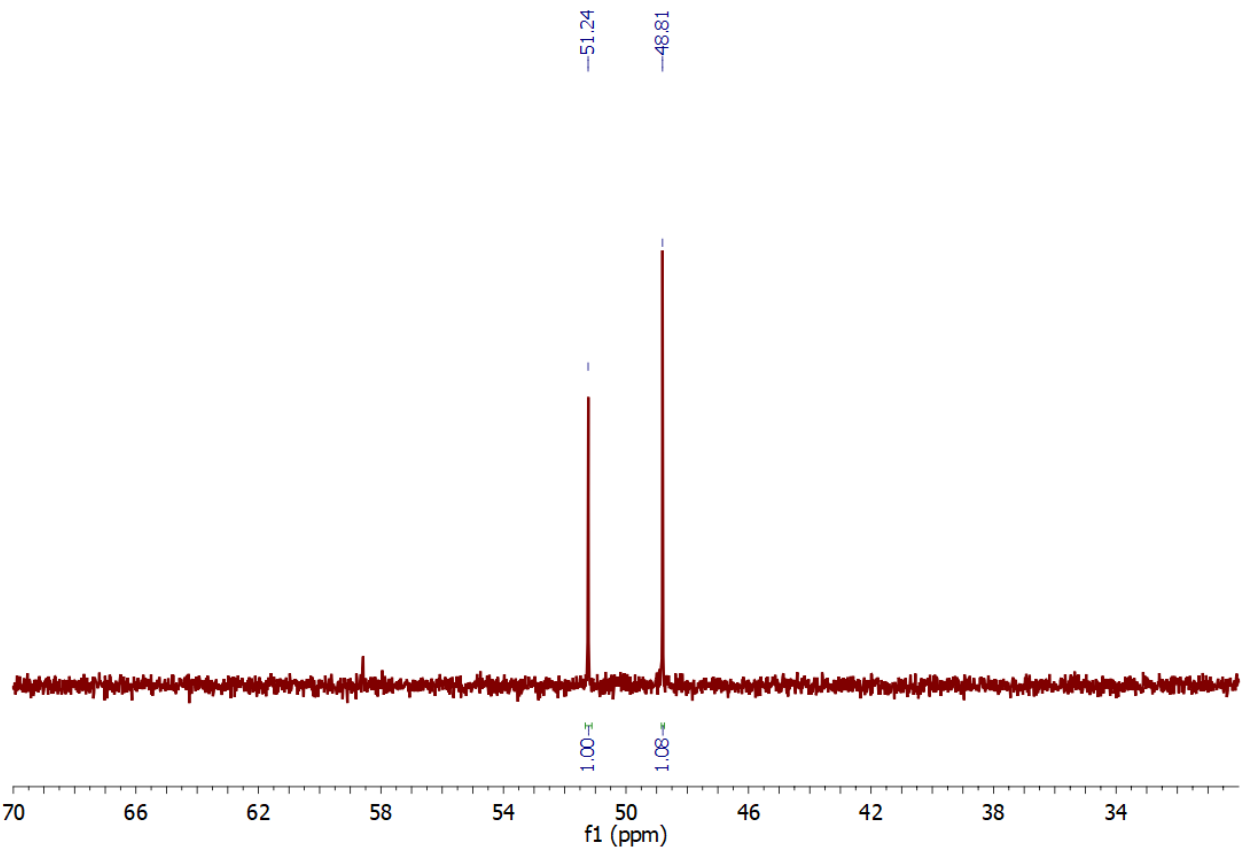

Figure S8. $^{31}P\{^{1}H\}$ NMR (283 MHz) spectrum of **1-CO·H_2BAr^F** in benzene-d_6 at 23 ºC.

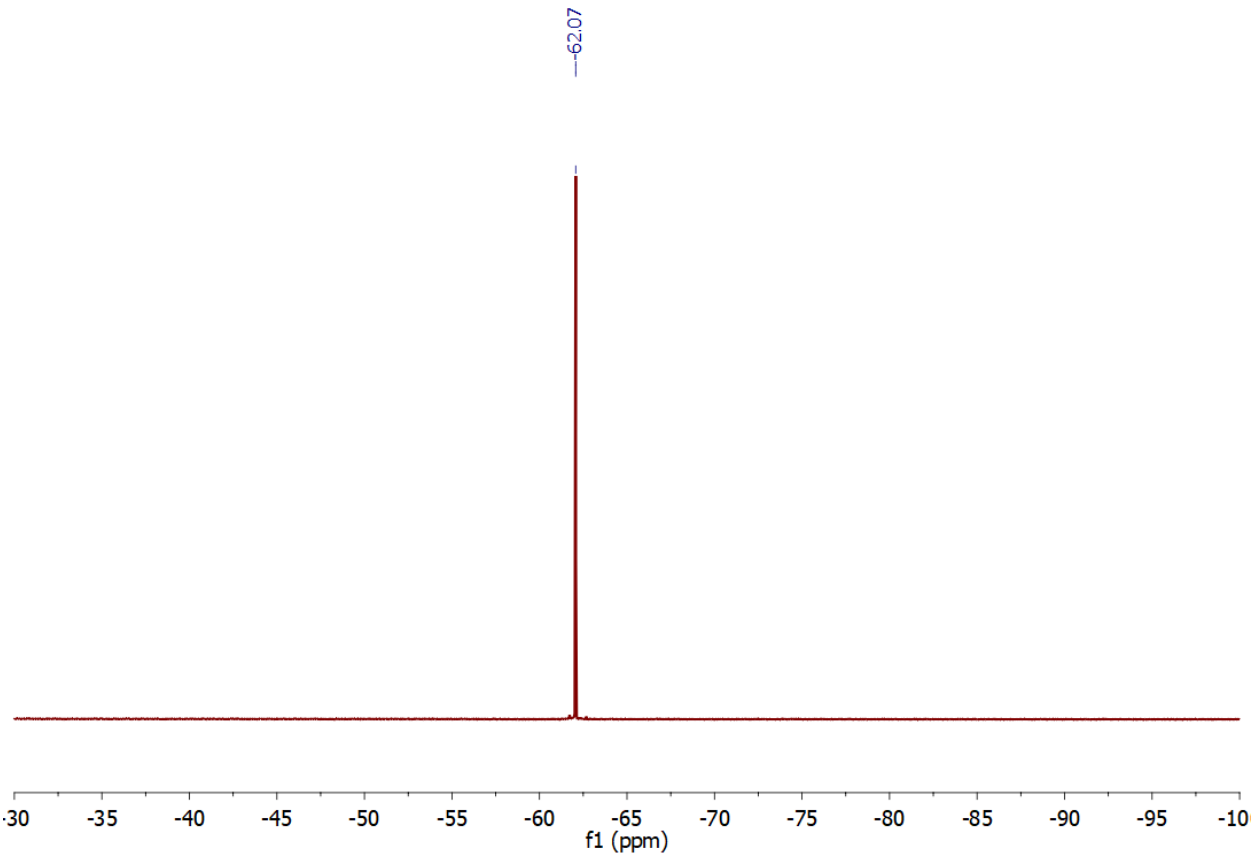

Figure S9. $^{19}F\{^{1}H\}$ NMR (659 MHz) spectrum of **1-CO·H_2BAr^F** in benzene-d_6 at 23 ºC.

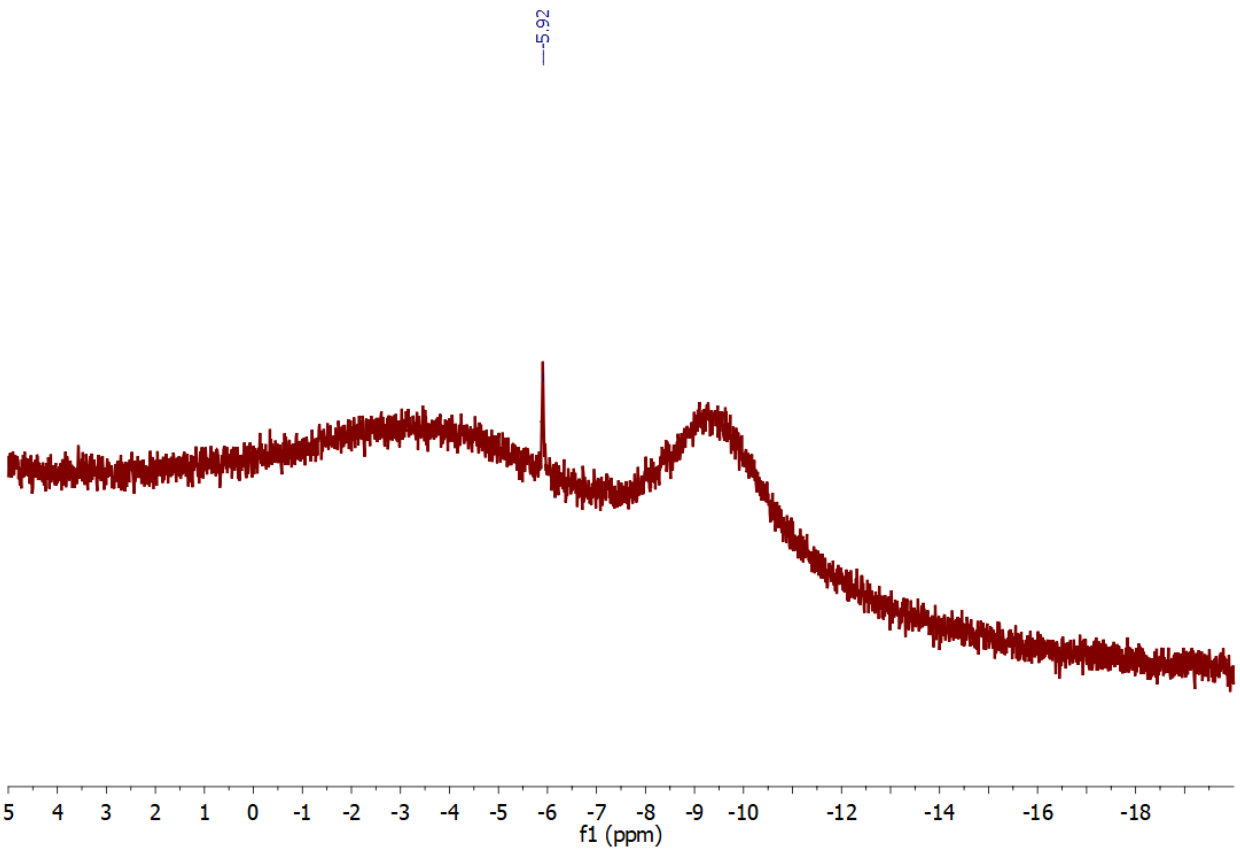

Figure S10. $^{11}B\{^{1}H\}$ NMR (225 MHz) spectrum of **1-CO·H_2BAr^F** in benzene-d_6 at 23 ºC.

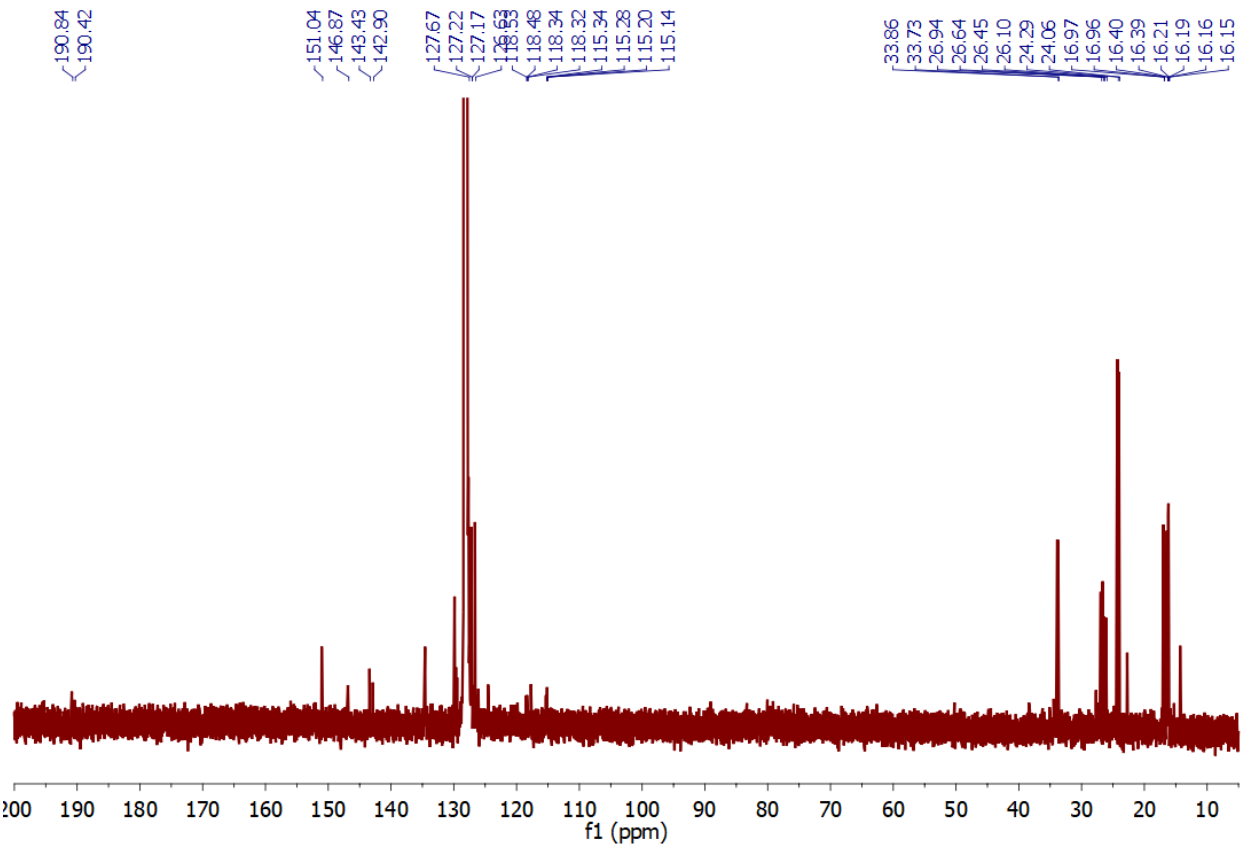

Figure S11. $^{13}C\{^{1}H\}$ NMR (176 MHz) spectrum of **1-CO•H_2BAr^F** in benzene-d_6 at 23 ºC.

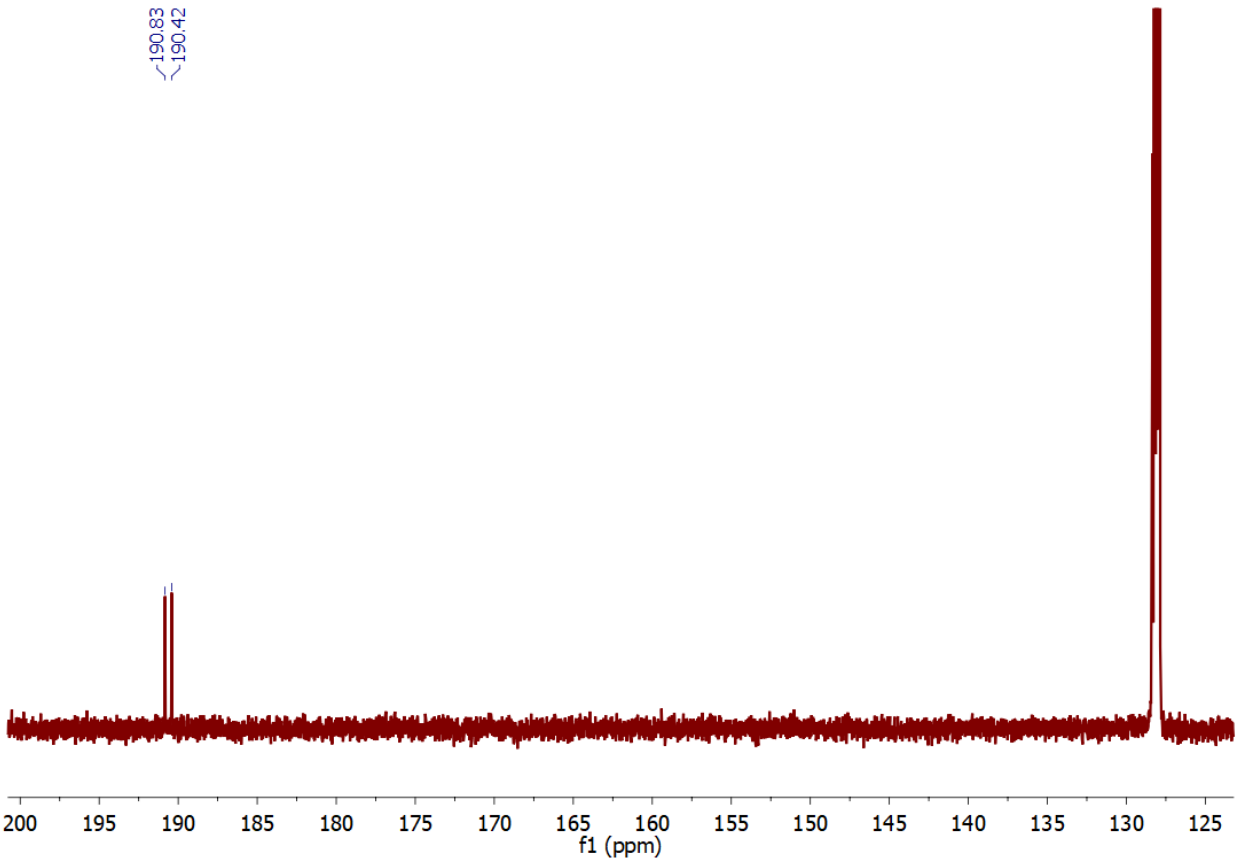

Figure S12. $^{13}C\{^{1}H\}$ NMR (176 MHz, downfield region) spectrum of **1-^{13}CO•H_2BAr^F** prepared with isotopically-enriched **1-^{13}CO**.

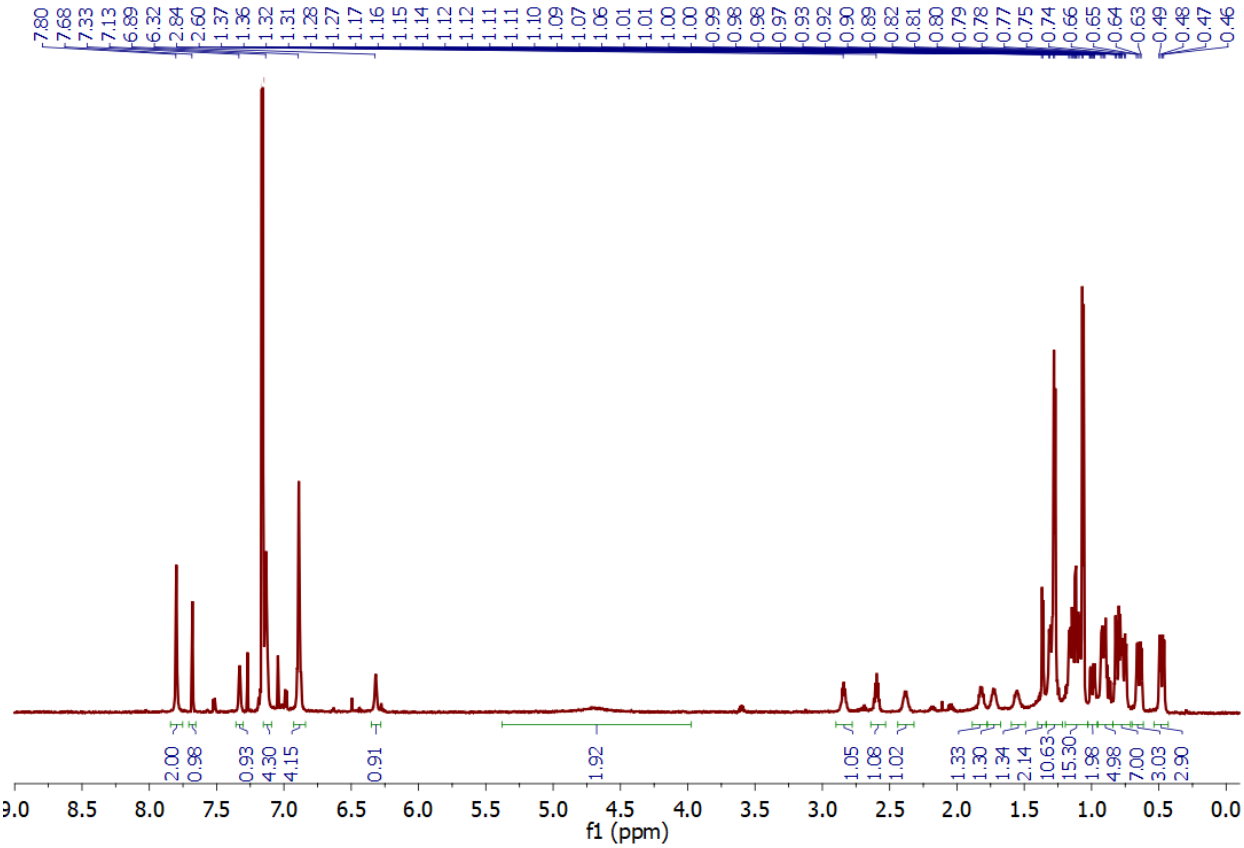

Figure S13. ^{1}H NMR (700 MHz) spectrum of **1-H$_2$BAr^F** in benzene-d_6 at 23 ºC.

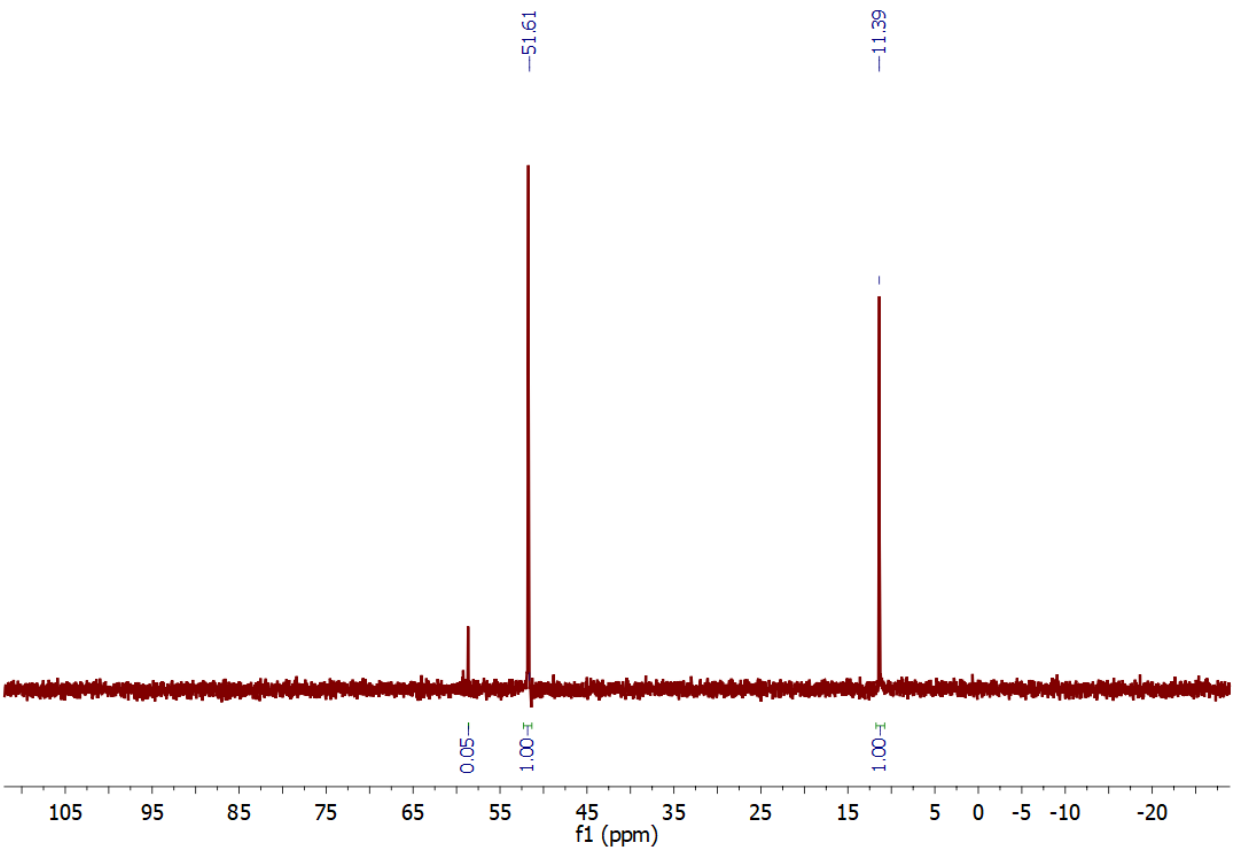

Figure S14. $^{31}P\{^{1}H\}$ (283 MHz) NMR spectrum of **1-H_2BAr^F** in benzene-d_6 at 23 ºC.

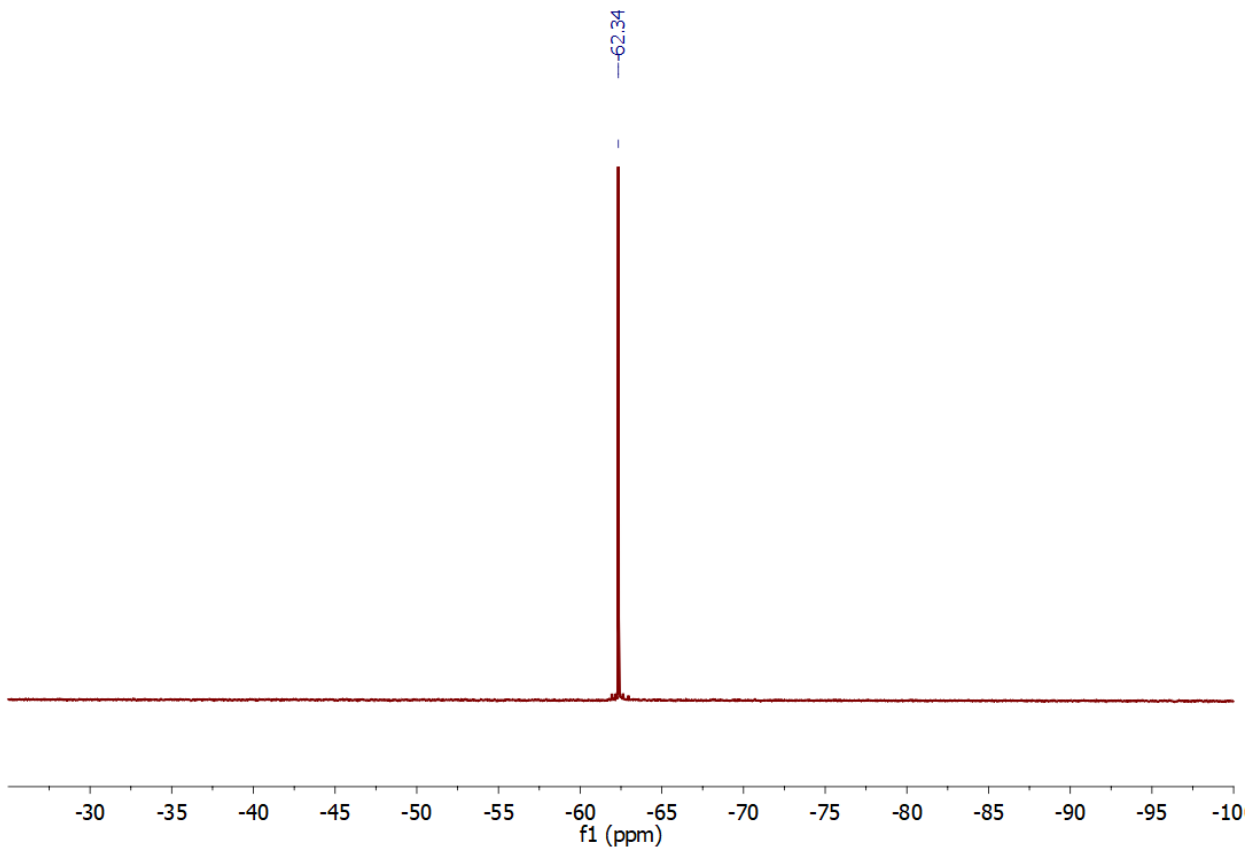

Figure S15. $^{19}F\{^{1}H\}$ NMR (659 MHz) spectrum of **1-H_2BAr^F** in benzene-d_6 at 23 ºC.

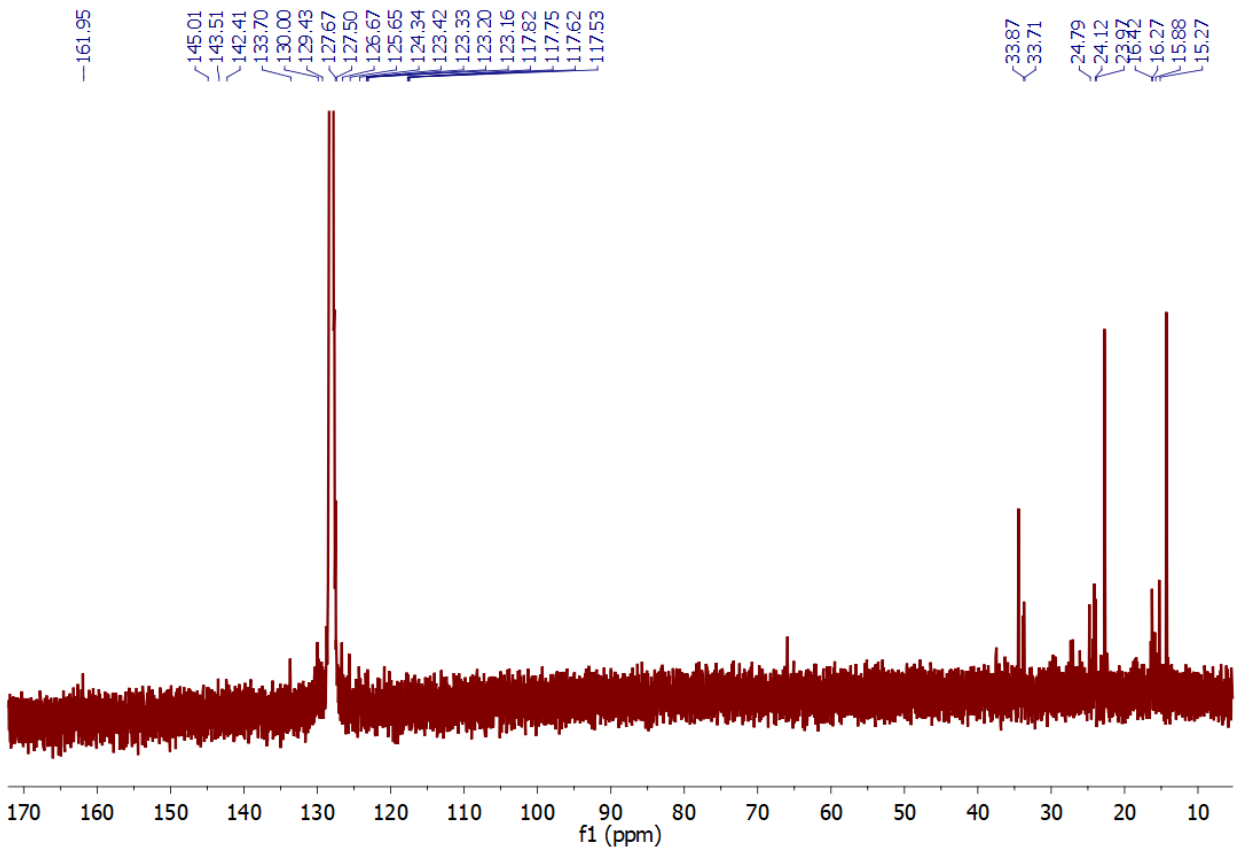

Figure S16. $^{13}C\{^{1}H\}$ NMR (176 MHz) spectrum of **1-H_2BAr^F** in benzene-d_6 at 23 ºC.

Reaction of **1-BMes** with 4 atm of H_2

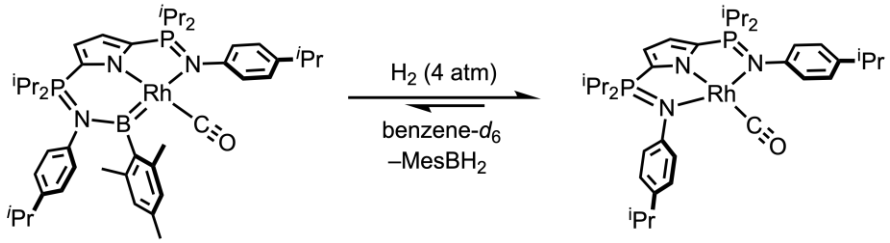

1-BMes **1-CO**

In a glovebox, a J. Young NMR tube was charged with **1-BMes** (0.010 g, 0.012 mmol) and dissolved in 0.6 mL of benzene-d_6. The tube was sealed and connected to a high-vacuum line where it was degassed by three freeze–pump–thaw cycles. While the contents of the tube were frozen, H_2 gas was introduced. The tube was sealed and warmed to ambient temperature, bringing the internal pressure of H_2 to approximately 4

atm. The tube was inverted at a rate of 20 min^{-1} to ensure adequate mixing. Formation of **1-CO** was observed by ^{1}H and ^{31}P NMR spectroscopy after 10 minutes.

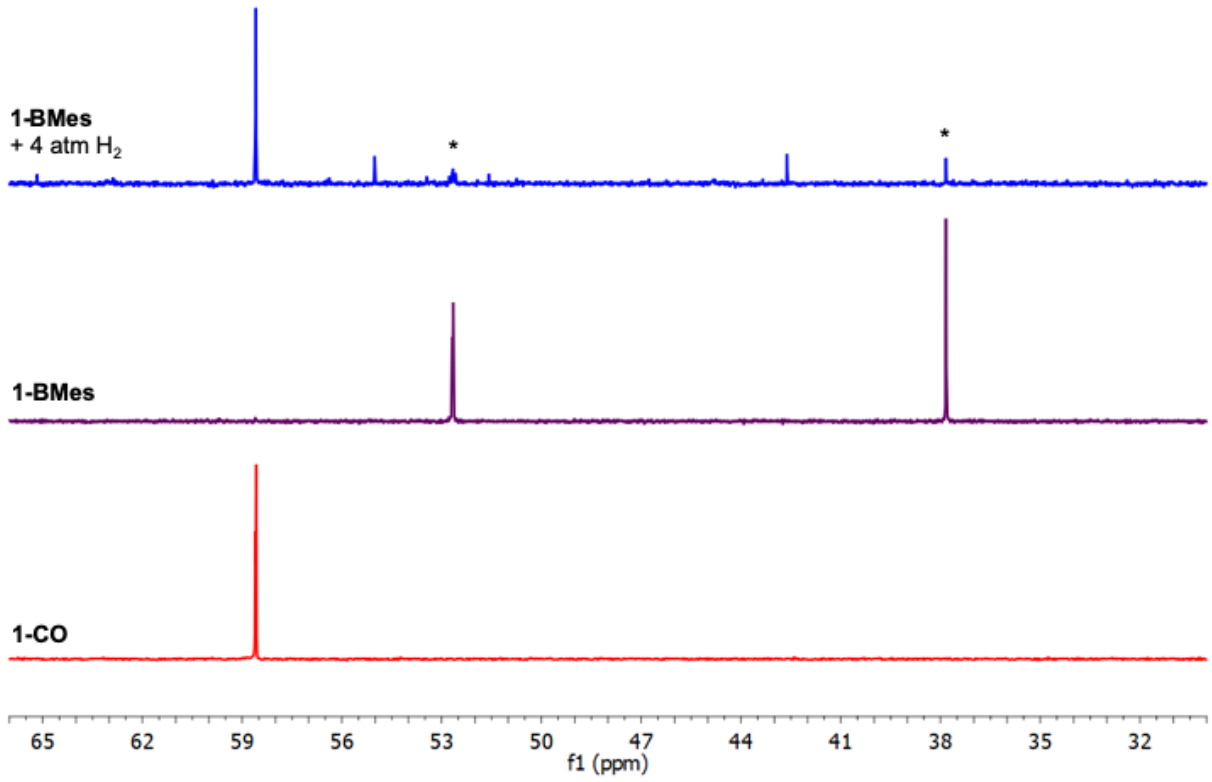

Figure S17. $^{31}P\{^{1}H\}$ NMR (283 MHz) spectra of **1-BMes** + 4 atm of H_2 in benzene-d_6. Authentic $^{31}P\{^{1}H\}$ NMR spectra of **1-BMes** and **1-CO** are shown for comparison. Peaks corresponding to residual **1-BMes** are marked (*) with an asterisk.

Reaction of **1-CO** with 1:1 H_2BMes/D_2BMes

In a 20 mL scintillation vial, a benzene-d_6 solution of mesitylborane (0.002 g, 0.014 mmol, 0.5 equivalents) and mesitylborane-d_2 (0.002 g, 0.014, 0.5 equivalents) were combined with **1-CO** (0.020 g, 0.029 mmol, 1 equivalent). The mixture was briefly agitated and then transferred into a J. Young NMR tube and sealed. The procedure was repeated without **1-CO** and monitored. No HD gas was observed in the absence of a rhodium complex.

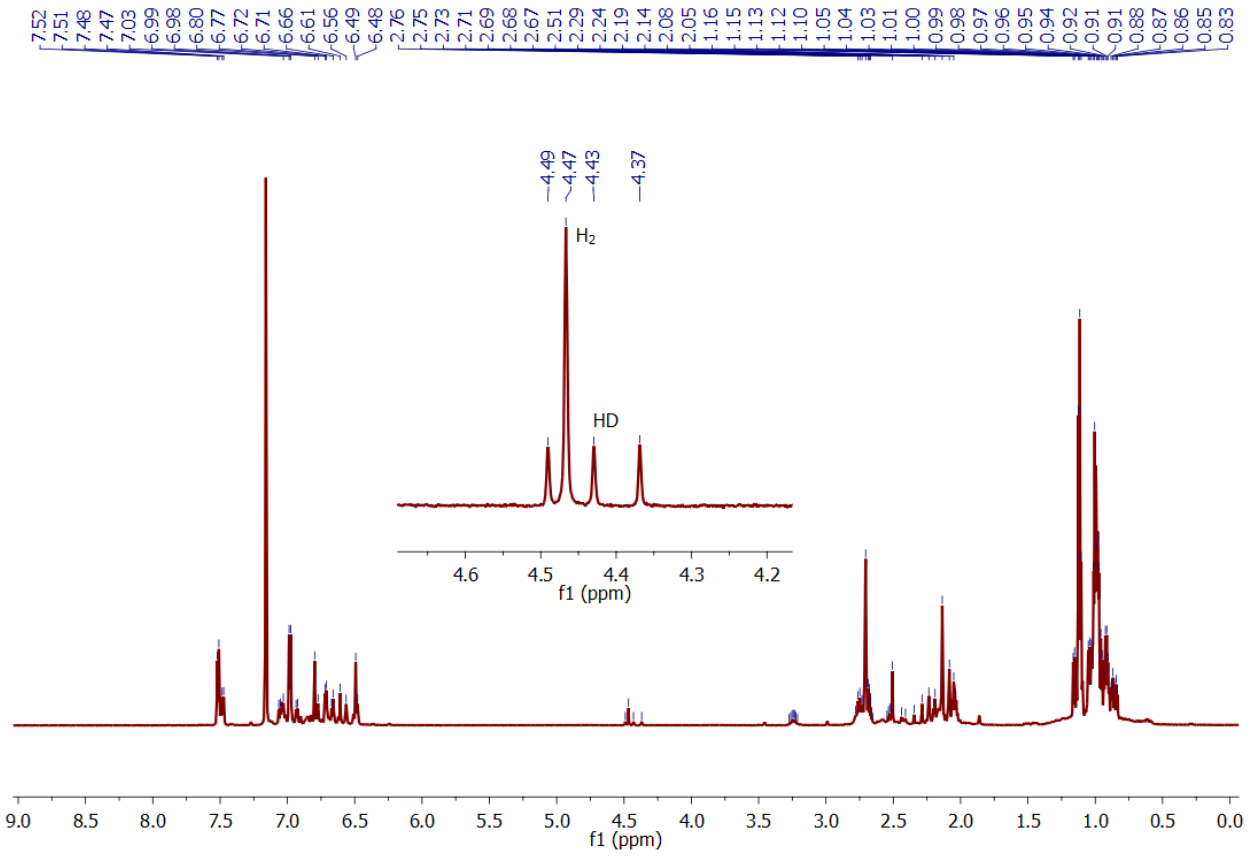

Figure S18. ^{1}H NMR (700 MHz) spectrum of **1-CO** + 1:1 mixture of mesitylborane and mesitylborane-d_2. Inset: enlarged region showing H_2 and HD gas in benzene-d_6.

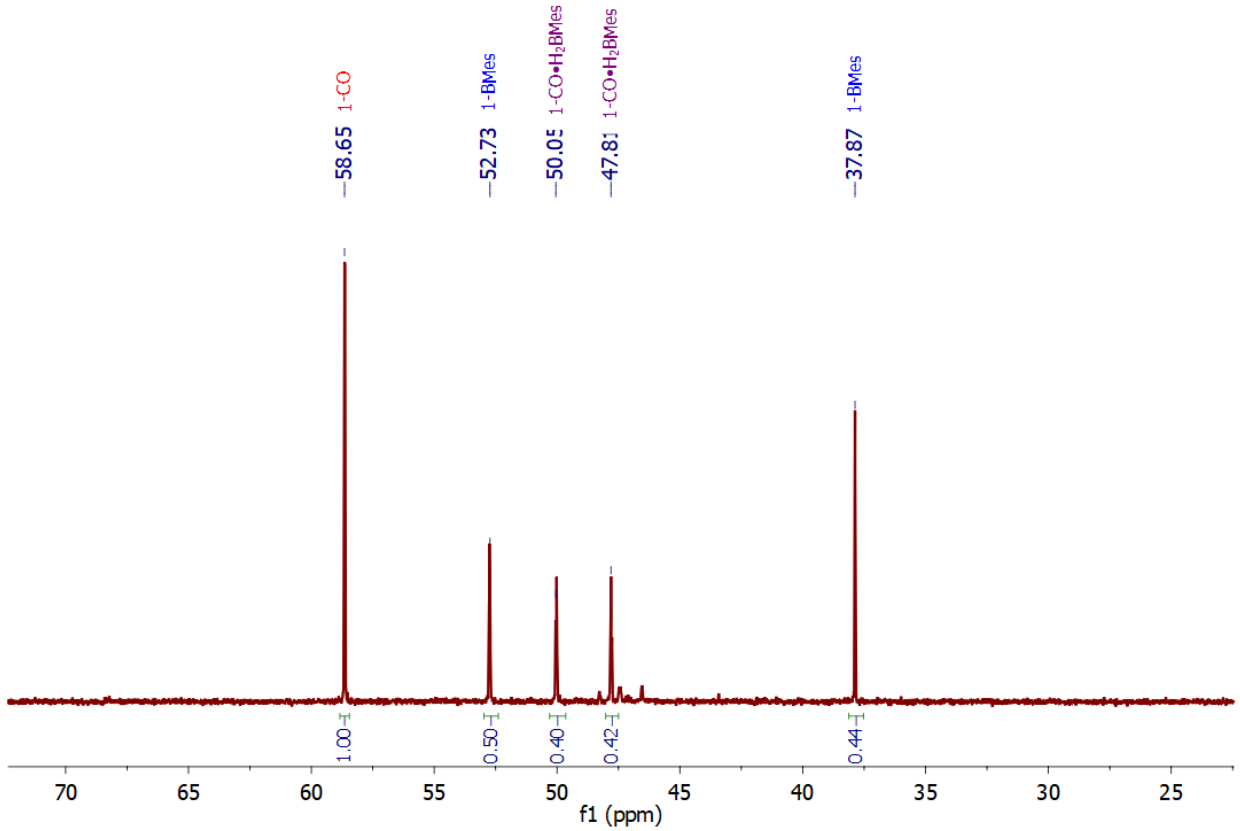

Figure S19. $^{31}P\{^{1}H\}$ NMR (283 MHz) spectrum of **1-CO** + 1:1 mesitylborane and mesitylborane-d_2. Here, "**1-CO·H$_2$BMes**" could theoretically be any of the isotopologues **1-CO·H$_2$BMes/1-CO·D$_2$BMes/1-CO·HDBMes**. The mixture of **1-CO/1-CO·H$_2$BMes/1-BMes** is approximately 1:1:1.

Reaction of **1-BMes** with Pinacol

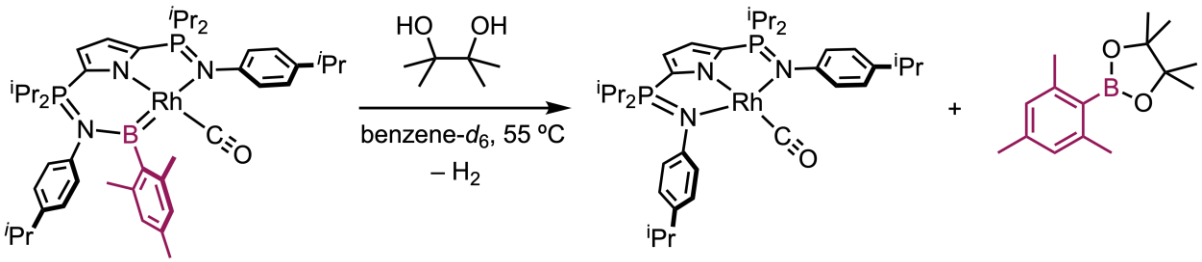

1-BMes **1-CO**

A J. Young NMR tube was charged with 0.011 g (0.013 mmol, 1 equivalent) of **1-BMes**, 1 equivalent of pinacol (0.0015 g, 0.013 mmol), and 0.6 mL of benzene-d_6. The tube was sealed and heated at 55 °C with periodic monitoring by NMR spectroscopy. After 6 days,

1-CO had formed in over 95% yield as determined by ^{1}H and ^{31}P NMR spectroscopy. During the reaction, the ^{1}H NMR spectrum of the reaction mixture showed trace amounts of H_2 gas.

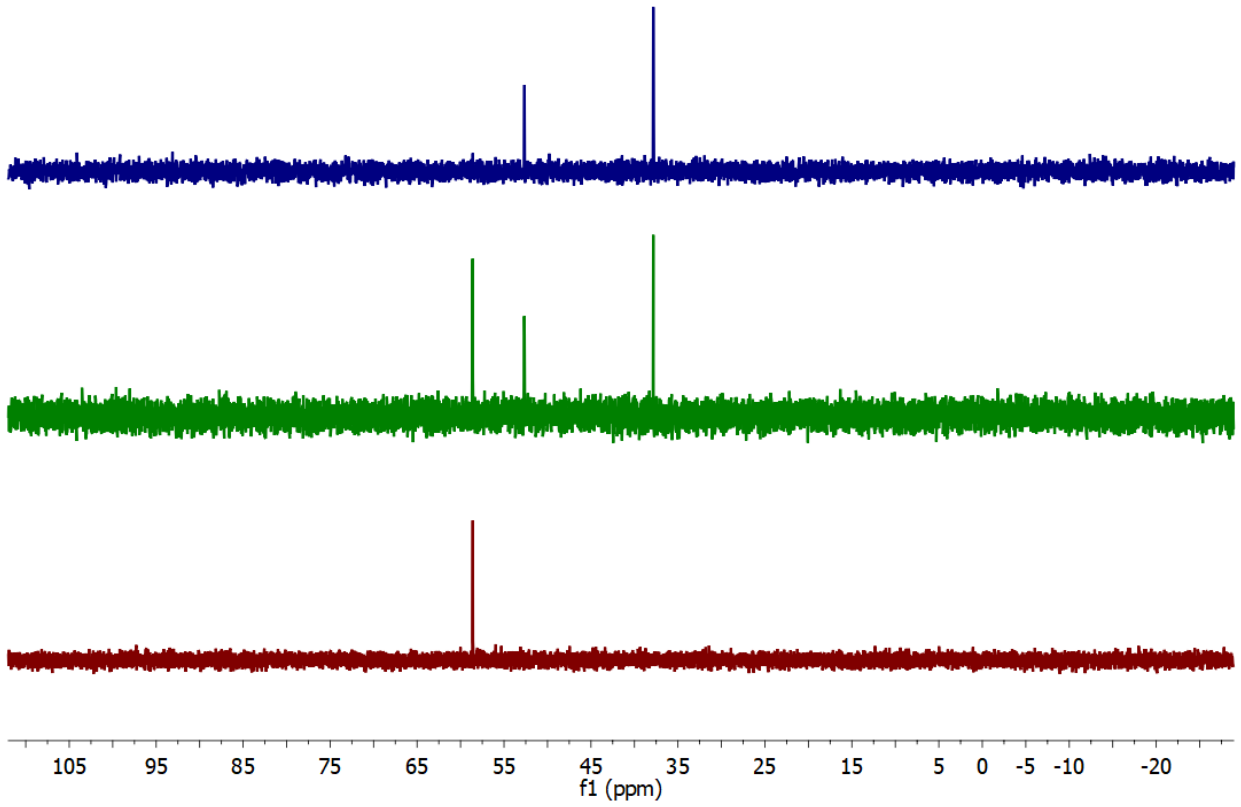

Figure S20. Stacked ^{31}P{^{1}H} NMR (283 MHz) spectra of **1-BMes** + pinacol. Blue: 1 hour; Green: 1 day; Red: 6 days. The bottom spectrum (red) is in accord with an authentic sample of **1-CO**.

IV. Variable Temperature NMR Spectroscopic Data

A J. Young NMR tube was charged with 0.011 g of **1-CO·H$_2$BArF** and 0.6 mL of toluene-d_8 and sealed. ^{1}H NMR spectra were first recorded at 22 ºC, and then at –80 ºC, rising in temperature to 22 ºC. The coalescence temperature T_{coal} was determined by careful inspection of the ^{1}H NMR spectra. At –25 ºC, the resonances assigned to Rh–*H* and B–*H* had disappeared into the baseline completely. The barrier for interconversion was calculated using equation S1.

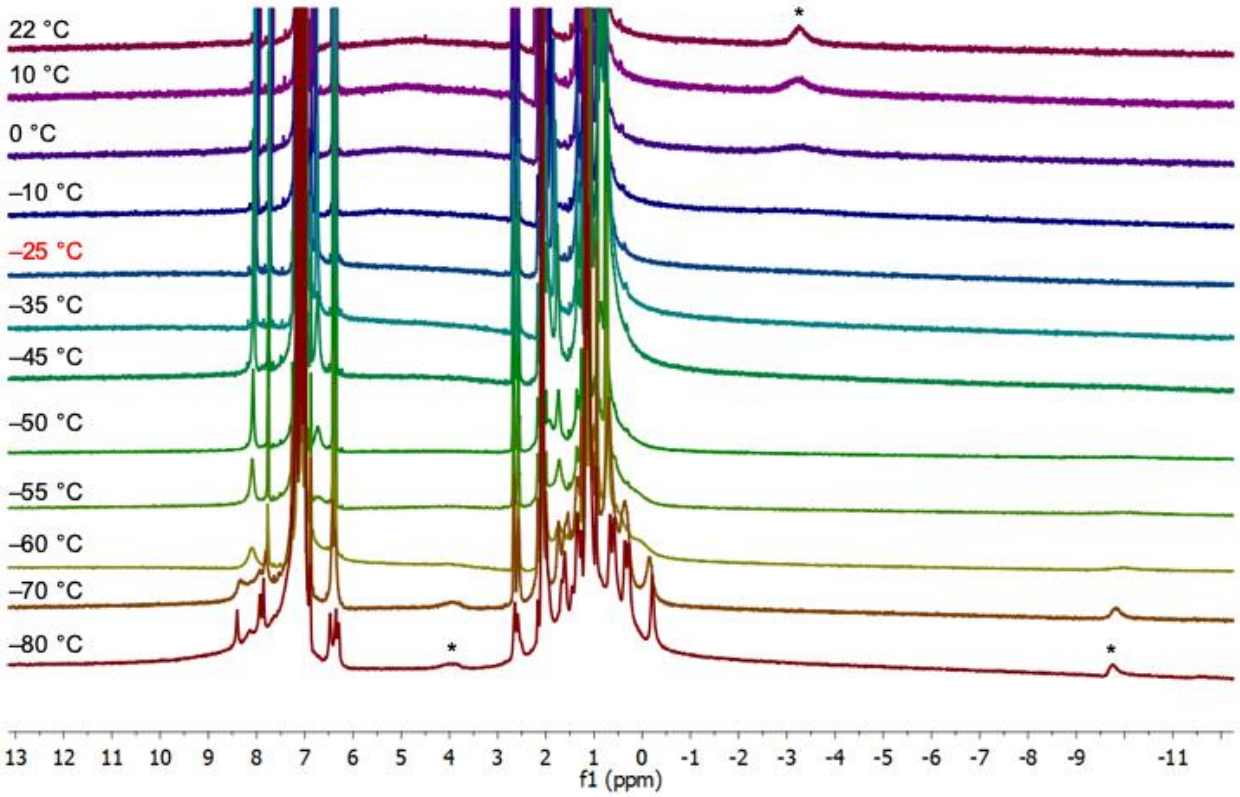

Figure S21. Variable temperature ^{1}H NMR (700 MHz) spectra of **1-CO·H_2BAr^F** in toluene-d_8. The peaks corresponding to the borane BH_2 protons are marked with an asterisk (*) and the coalescence temperature (–25 ºC) is highlighted in red.

Determination of $\Delta G^{\ddagger}_{coal}$ from Variable Temperature NMR spectroscopy

The coalescence temperature (T_{coal}) was determined by careful inspection of the ^{1}H NMR spectra in toluene-d_8 at a range of temperatures. At –25 ºC, the peaks corresponding to the B–*H* and Rh–*H* protons vanished and the broad peak corresponding to the BH_2 moiety had not yet appeared. Here, $\Delta\nu$ is the maximum peak separation in Hz. The $\Delta G^{\ddagger}$ was calculated according to equation S1 at the coalescence temperature (–25 ºC) to be 9.9(4) kcal mol^{-1}.[6]

$$\Delta G^{\ddagger}_{coal}\,(\text{kcal mol}^{-1}) = \frac{1.914 \times 10^{-2}(T_{coal})[9.972+\log\frac{T_{coal}}{\Delta\nu}]}{4.184} \qquad \text{(S1)}$$

V. Crystallographic Details

X-Ray Diffraction Techniques. All structures were collected on a Rigaku SuperNova diffractometer equipped with a Dectris Pilatus 3R 200K-A hybrid-pixel-array detector, a four-circle κ goniometer, sealed graphite-monochromated Mo Kα (λ = 0.71073 Å) and Cu Kα (λ = 1.54178 Å) X-ray sources, and an Oxford cryostream-cooling device fixed at 100 K. Single crystals suitable for X-ray diffraction studies were mounted on a MiTiGen cryo-loop using desiccated Paratone–*N* oil stored in a glovebox.

The structures were solved by the Intrinsic Phasing methods and refined by least-squares methods using SHELXT-2014 and SHELXL-2014 with the OLEX2 interface.[7-9] The program PLATON was employed to confirm the absence of higher symmetry space groups.[10] All non-H atoms were located in difference Fourier maps, and then refined anisotropically. Outlier reflections were omitted from refinement when appropriate. Hydrogen atoms on C atoms were placed at idealized positions and refined using a riding model. The isotropic displacement parameters of all hydrogen atoms were fixed to 1.2 times the atoms they are linked to (1.5 times for methyl groups). Crystallographic refinement details, including disorder modeling and software employed, have been delineated within each crystallographic information file (*.cif). Molecular graphics were generated using ORTEP and Adobe Illustrator.

Further details on particular structures are noted below:

1-BMes. The unit cell contained two unique molecules oriented in a head-to-tail arrangement. A short contact (2.193 Å) was located between the carbonyl oxygen atom of one molecule and the pyrrole C–H atom of another.

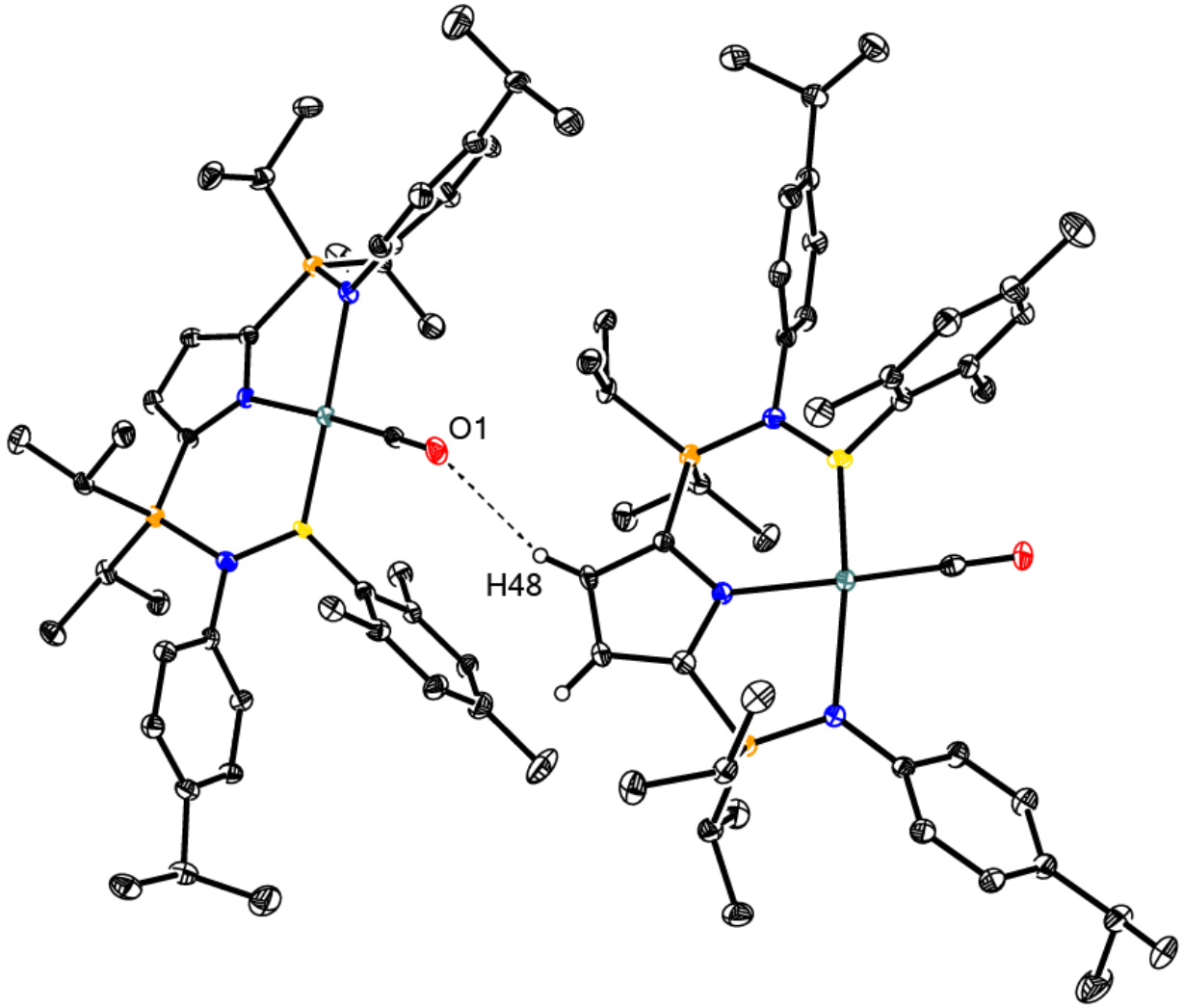

Figure S22. Unit cell of **1-BMes** with 30% probability ellipsoids. Short contact (2.193 Å) between O1 and H48 is shown.

Table S1. Single crystal X-ray diffraction details of reported complexes.

	1-BMes	**1-CO•H_2BAr^F**
CCDC Entry	198537	1985379
Crystal Size (mm)	0.20 × 0.10 × 0.05	0.25 × 0.25 × 0.25
Moiety Formula	$C_{44}H_{63}BN_3OP_2Rh$	$C_{43}H_{57}BF_6N_3OP_2Rh•C_6H_6$
Formula weight (g/mol)	825.63	999.68
λ (nm)	1.54178	0.71073
T (K)	100(2)	100(2)
Crystal System	Triclinic	Monoclinic
Space group (*Z*)	P–1 (4)	*I*2/*a* (8)
a (Å)	14.5167(3)	28.3648(5)
b (Å)	18.5067(4)	12.2130(1)
c (Å)	19.7008(6)	32.5843(5)
α (deg)	65.627(2)	90
β (deg)	88.777(2)	111.394(2)
γ (deg)	77.349(2)	90
Volume (Å^3)	4689.8(2)	10510.0(3)
Calc. *ρ* (g cm^{-3})	1.169	1.264
μ (mm^{-1})	3.831	0.443
Reflections	18596	11658
Completeness (to 2θ)	0.960	0.995
C–C Bond Precision (Å)	0.0093	0.0025
R_1, wR_2 [$I > 2\sigma(I)$]	0.0759, 0.2131	0.0261, 0.0657
Go on F^2	1.080	1.035

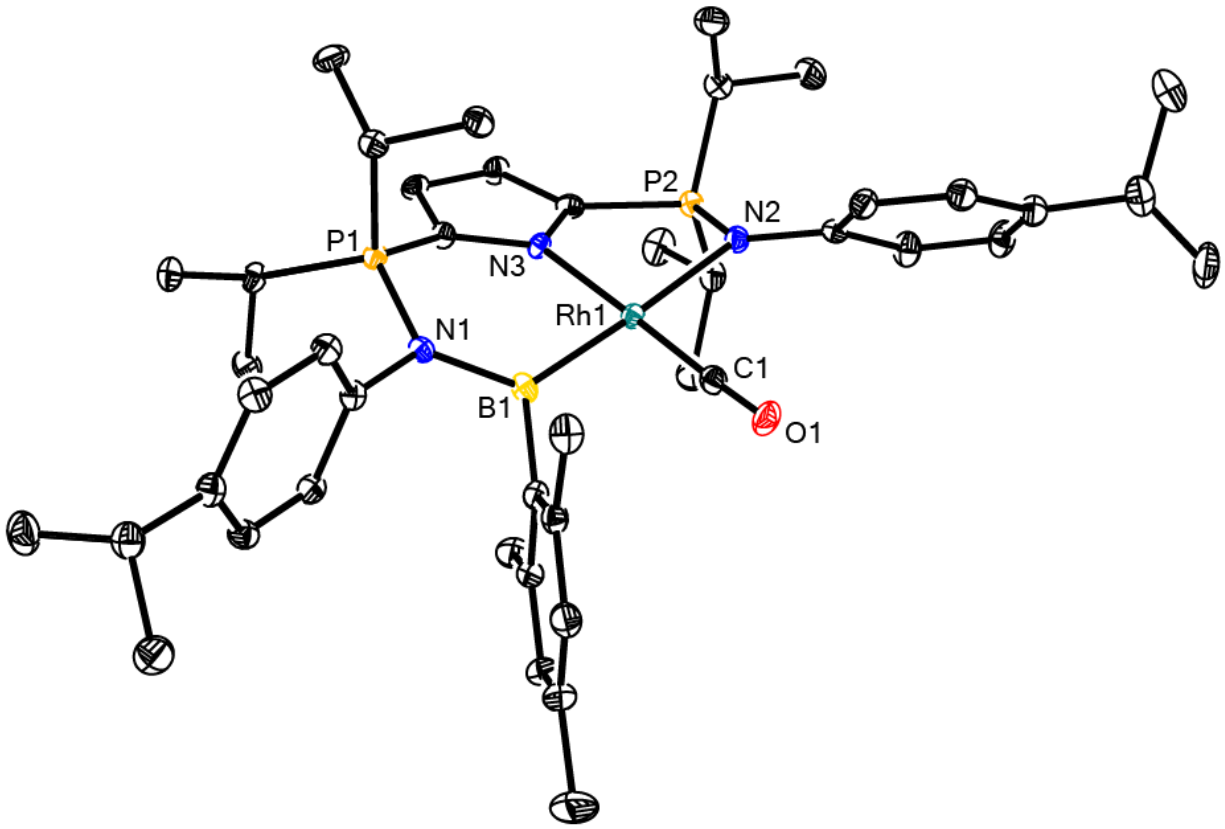

Figure S23. Molecular structure of **1-BMes** with 30% probability ellipsoids. Hydrogen atoms omitted for clarity.

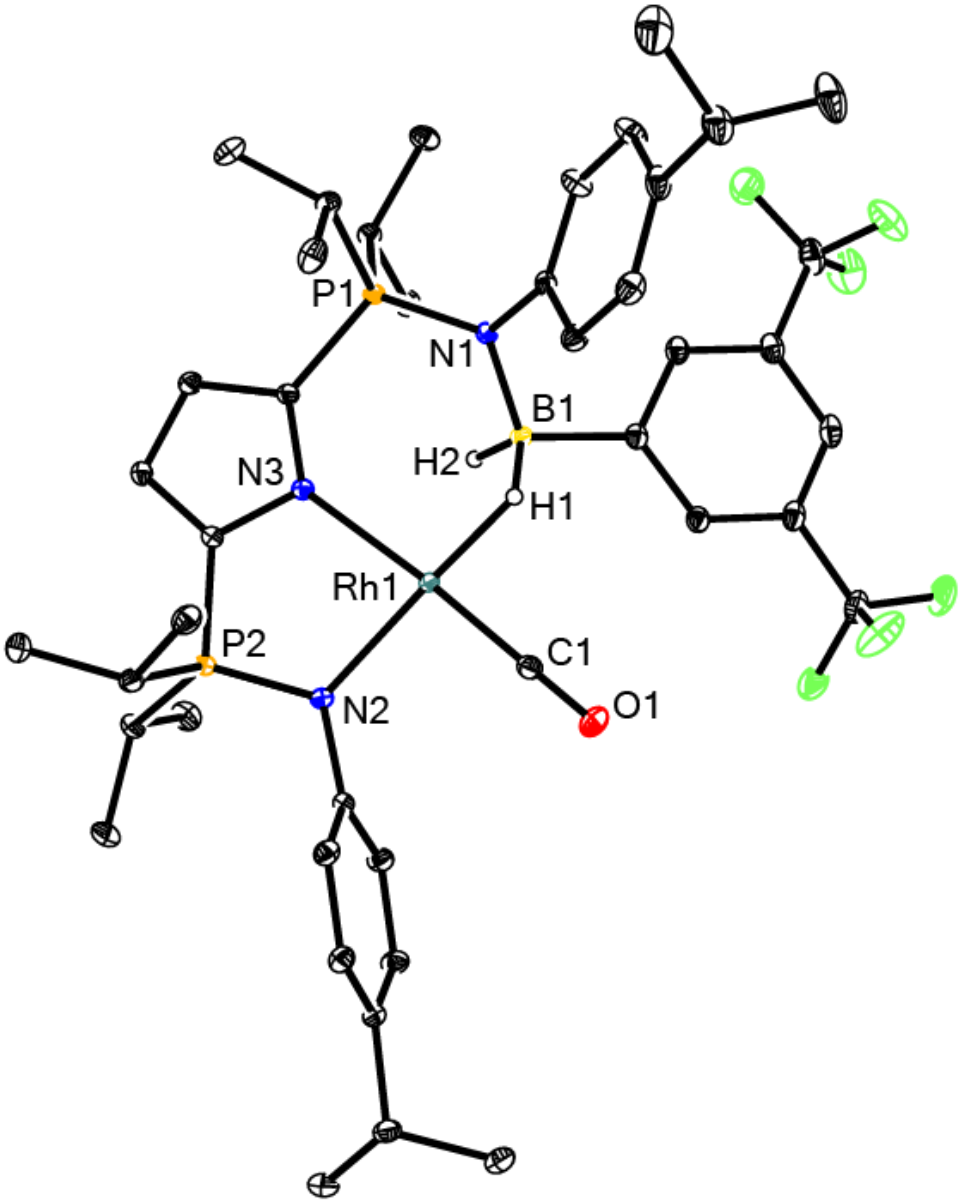

Figure S24. Molecular structure of **1-CO·H_2BAr^F** with 30% probability ellipsoids. All hydrogen atoms except BH_2 and solvent molecules of recrystallization are omitted for clarity.

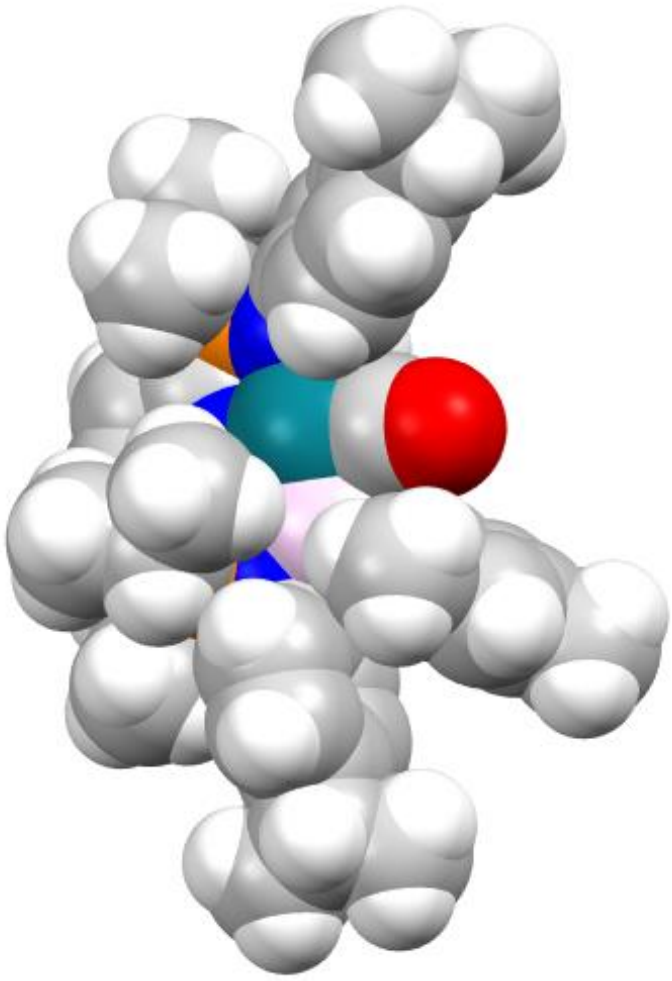

Figure S25. Space-filling model of **1-BMes** illustrating the steric shielding of the mesityl methyl groups.

VI. Computational Details

Density Functional Theory (DFT) calculations were carried out on the unmodified structure of **1-BMes** using the Gaussian 16 (revision B.01) computational suite.[11] Cartesian coordinates were obtained from X-ray diffraction analysis. Gas-phase geometry optimization was performed using the B3LYP functional,[12] employing the aug-cc-pVDZ basis set with associated pseudopotentials (Rh) for non C, H atoms (cc-pVDZ).[13] Visualization of optimized structures and rendering of molecular orbitals was performed using Gaussview.[14] Wiberg bond indices were determined using NBO 3.1,[15,16] also using the B3LYP/aug-cc-pVDZ level of theory.

Sample Geometry Optimization and NBO Calculation Input File

B3LYP genecp guess=read pop=(full, nbo, savenbos) gfinput

1-BMes

0 1

Rh	0.79177806	0.14736201	-0.11382101
P	-2.00976614	-2.17552716	-0.60185805
P	3.23365523	-1.84708013	0.82912706
O	1.25883109	3.05659622	-0.58938804
N	-2.29621916	-0.53269104	-0.23770302
N	0.59328604	-1.90410414	0.21987502
N	3.00672121	-0.42268603	0.05699600
C	-0.47404803	-2.74148419	0.10623201
C	-0.11425501	-4.06180529	0.45904503
H	-0.74773405	-4.94559135	0.45848003
C	-3.69491326	-0.13873801	-0.32263802
C	-1.98429014	-2.46844418	-2.45260318
H	-3.00140122	-2.20735216	-2.78646520
C	-3.29404824	-3.32957724	0.11680901
H	-2.80969420	-4.30054731	-0.08403901
C	1.64013612	-2.66735919	0.65103905
C	-4.43092032	0.14061901	0.83817806
H	-3.94133928	0.07285101	1.80845913
C	-1.80525413	1.90742314	0.44309103
C	-2.16567515	2.91720821	-0.47890803
C	-5.76897342	0.52398204	0.75807705
H	-6.30553147	0.74274405	1.68427712
C	1.24466709	-4.00801629	0.81430006
H	1.86294414	-4.84088035	1.14174608
C	-4.33433431	-0.00436300	-1.56090411
H	-3.77445927	-0.17318801	-2.48098718
C	-1.88205714	2.21306316	1.82870313
B	-1.20590609	0.49889804	-0.00980600
C	-3.41328325	-3.17247423	1.64054512
H	-2.43039517	-3.15507023	2.13154115
H	-3.98394529	-4.02280229	2.04692715
H	-3.95206829	-2.25229116	1.90375714
C	-5.68044641	0.37084103	-1.63307412
H	-6.15285442	0.46816003	-2.61442719
C	4.49774933	-2.99510821	0.05654800
H	4.26746531	-3.97894528	0.50312904
C	-4.66664133	-3.34798224	-0.57235104
H	-5.23898738	-2.43299217	-0.37199703
H	-5.24488338	-4.20081630	-0.18115601
H	-4.59313733	-3.47456025	-1.66244312
C	4.14990430	0.96184207	-1.57660512
H	3.39692425	0.64373005	-2.30030416
C	-1.42989710	1.20527409	2.86320421
H	-2.03670015	0.28291002	2.84997120

H	-1.48170411	1.62117712	3.88075828
H	-0.39231003	0.88827406	2.66152219
C	-6.42698945	0.64091105	-0.47920903
C	4.06822629	0.45429503	-0.26435302
C	1.03817107	1.93168414	-0.39983303
C	6.12816544	2.29486216	-1.03523108
C	5.15289037	1.85856813	-1.94542214
H	5.17634837	2.23202216	-2.97371621
C	4.25761230	-3.07558522	-1.45823710
H	3.21733123	-3.34476924	-1.69270012
H	4.91780835	-3.84052328	-1.89832913
H	4.47693832	-2.11228915	-1.94250814
C	-0.97611907	-1.54019411	-3.14400023
H	-1.16113108	-0.48104003	-2.92090021
H	-1.04093307	-1.68639412	-4.23436330
H	0.05354000	-1.75836213	-2.82385521
C	-2.61411619	4.16596930	-0.02131600
H	-2.87689021	4.93420535	-0.75588205
C	3.63838826	-1.76108213	2.66418119
H	4.65040534	-1.32441210	2.70125119
C	6.04171942	1.79931113	0.27477402
H	6.76492951	2.12218815	1.02884607
C	-1.71639312	-3.94354228	-2.78977320
H	-0.73447805	-4.26639531	-2.41147318
H	-1.71383112	-4.06812229	-3.88431628
H	-2.48207818	-4.62249633	-2.38485317
C	3.67363726	-3.14017722	3.33864324
H	3.94337629	-3.02608122	4.40143032
H	4.41223632	-3.81841828	2.88409921
H	2.68704519	-3.62788426	3.29798924
C	-2.05708015	2.68325819	-1.96973014
H	-2.01672015	3.63462426	-2.52164918
H	-2.92131521	2.11700315	-2.35618417
H	-1.15038508	2.10878015	-2.21903116
C	5.03455436	0.90940707	0.65715205
H	4.98487936	0.58406504	1.69775012
C	-2.71873520	4.46157932	1.34010010
C	5.95509141	-2.63418919	0.38309903
H	6.22481845	-1.64742812	-0.02074200
H	6.62814349	-3.38003824	-0.07093801
H	6.15665545	-2.62590619	1.46496910
C	-2.33891717	3.46564925	2.25125816
H	-2.38471917	3.67760227	3.32494524
C	-7.88682158	1.06498808	-0.57183904
H	-8.14993956	1.06778308	-1.64423312
C	2.66104919	-0.80787906	3.36530124
H	1.63652012	-1.21205709	3.35031024
H	2.63212219	0.17883001	2.88163721
H	2.96006421	-0.67514605	4.41779732
C	-8.09976356	2.49355618	-0.03948600
H	-9.14839765	2.80610820	-0.17512001

H	-7.45472756	3.21577323	-0.56387204
H	-7.86840055	2.55945719	1.03673907
C	-8.82288962	0.06540400	0.13058401
H	-8.62344361	0.02101600	1.21445409
H	-8.70144963	-0.95179407	-0.27512502
H	-9.87670674	0.36175003	-0.00042600
C	-3.18769223	5.81414341	1.82255713
H	-2.37545517	6.36453744	2.32872617
H	-4.01278329	5.72174239	2.54918718
H	-3.54188425	6.43903845	0.98857007
C	7.21381353	3.27696824	-1.45595410
H	7.05026950	3.49080525	-2.52718018
C	7.10681151	4.61334833	-0.69942705
H	6.11024142	5.06429037	-0.82767406
H	7.86037859	5.33229239	-1.06328508
H	7.27377852	4.47509132	0.38228403
C	8.62419965	2.67614719	-1.31743310
H	8.86015766	2.44673018	-0.26434302
H	9.38982668	3.38142124	-1.68266812
H	8.71831461	1.74071813	-1.89205213

C H 0
cc-pvdz
****
P N O B 0
aug-cc-pvdz
****
Rh 0
S 10 1.00

2.289320E+02	5.680000E-04
1.990870E+01	-4.680300E-02
1.244680E+01	2.723670E-01
7.778210E+00	-2.301680E-01
4.580060E+00	-5.095540E-01
1.290680E+00	8.098500E-01
5.934140E-01	4.978760E-01
1.491580E-01	3.315400E-02
7.195300E-02	-1.151300E-02
3.175200E-02	4.206000E-03

S 10 1.00

2.289320E+02	-1.860000E-04
1.990870E+01	1.518000E-02
1.244680E+01	-9.113000E-02
7.778210E+00	9.119900E-02
4.580060E+00	1.503790E-01
1.290680E+00	-3.344630E-01
5.934140E-01	-3.074430E-01
1.491580E-01	2.695540E-01
7.195300E-02	6.048640E-01
3.175200E-02	3.070670E-01

S 10 1.00
2.289320E+02 -2.440000E-04
1.990870E+01 7.929000E-03
1.244680E+01 -9.389300E-02
7.778210E+00 7.936000E-03
4.580060E+00 5.418830E-01
1.290680E+00 -1.497488E+00
5.934140E-01 4.948550E-01
1.491580E-01 1.990527E+00
7.195300E-02 -1.226037E+00
3.175200E-02 -5.093060E-01
S 10 1.00
2.289320E+02 -7.250000E-04
1.990870E+01 5.993000E-02
1.244680E+01 -3.549510E-01
7.778210E+00 3.902970E-01
4.580060E+00 5.857430E-01
1.290680E+00 -3.302856E+00
5.934140E-01 3.625717E+00
1.491580E-01 -1.236749E+00
7.195300E-02 -1.007047E+00
3.175200E-02 1.352346E+00
S 1 1.00
3.175200E-02 1.000000E+00
S 1 1.00
1.400000E-02 1.000000E+00
P 9 1.00
2.421170E+01 -1.579000E-03
1.513310E+01 2.719800E-02
6.447200E+00 -1.914630E-01
1.777760E+00 4.476580E-01
8.990200E-01 4.777240E-01
4.445220E-01 2.058190E-01
1.886740E-01 2.435200E-02
7.851400E-02 -5.800000E-05
3.219500E-02 3.330000E-04
P 9 1.00
2.421170E+01 -1.320000E-04
1.513310E+01 -6.532000E-03
6.447200E+00 5.644500E-02
1.777760E+00 -1.610630E-01
8.990200E-01 -1.842580E-01
4.445220E-01 -3.361000E-02
1.886740E-01 3.445440E-01
7.851400E-02 5.595730E-01
3.219500E-02 2.467510E-01
P 9 1.00
2.421170E+01 1.470000E-04
1.513310E+01 -1.335300E-02
6.447200E+00 1.094800E-01
1.777760E+00 -3.362590E-01

```
   8.990200E-01   -3.686360E-01
   4.445220E-01    2.138540E-01
   1.886740E-01    6.803790E-01
   7.851400E-02    3.077610E-01
   3.219500E-02    1.258900E-02
P 9 1.00
   2.421170E+01    2.304000E-03
   1.513310E+01   -2.729700E-02
   6.447200E+00    1.976470E-01
   1.777760E+00   -8.063470E-01
   8.990200E-01   -3.874520E-01
   4.445220E-01    1.516827E+00
   1.886740E-01   -1.135820E-01
   7.851400E-02   -8.286130E-01
   3.219500E-02   -2.446000E-02
P 1 1.00
   3.219500E-02    1.000000E+00
P 1 1.00
   1.320000E-02    1.000000E+00
D 8 1.00
   2.949980E+01    1.677000E-03
   7.404370E+00   -1.843900E-02
   3.059590E+00    1.050760E-01
   1.582050E+00    2.937700E-01
   7.748340E-01    3.641780E-01
   3.630560E-01    2.972650E-01
   1.610470E-01    1.599580E-01
   6.562000E-02    3.867900E-02
D 8 1.00
   2.949980E+01   -1.786000E-03
   7.404370E+00    2.013000E-02
   3.059590E+00   -1.279690E-01
   1.582050E+00   -3.807800E-01
   7.748340E-01   -2.708410E-01
   3.630560E-01    2.651630E-01
   1.610470E-01    5.378200E-01
   6.562000E-02    2.758530E-01
D 8 1.00
   2.949980E+01    3.029000E-03
   7.404370E+00   -3.628200E-02
   3.059590E+00    2.815510E-01
   1.582050E+00    6.384210E-01
   7.748340E-01   -3.871850E-01
   3.630560E-01   -7.962390E-01
   1.610470E-01    3.375180E-01
   6.562000E-02    5.715430E-01
D 1 1.00
   6.562000E-02    1.000000E+00
D 1 1.00
   2.670000E-02    1.000000E+00
F 1 1.00
```

```
   1.960600E+00     1.000000E+00
 F 1 1.00
   5.553000E-01     1.000000E+00
 F 1 1.00
   2.095000E-01     1.000000E+00
 G 1 1.00
   1.190700E+00     1.000000E+00
 G 1 1.00
   5.001000E-01     1.000000E+00
 ****

Rh 0
ECP28MDF 4 28
G-Komponente
1
2 1.000000 0.000000
S-G
2
2 12.194816 225.312054
2 5.405137 32.441582
P-G
4
2 11.280755 52.872826
2 10.927248 105.745526
2 5.090117 8.619344
2 4.851832 16.973459
D-G
4
2 9.136337 25.108501
2 8.964808 37.695731
2 3.643612 4.202584
2 3.636007 6.292790
F-G
2
2 8.616228 -9.673568
2 8.629435 -12.899847


$NBO bndidx $END
```

Computational results for 1-BMes

Table S2. Comparison of DFT-calculated (B3LYP/aug-cc-pVDZ) and experimental structural parameters in **1-BMes**.

Parameter	Experimental	Calculated	% Difference
d(Rh1–B1) (Å)	2.024(5)	2.031	0.34%
d(P1–N1) (Å)	1.658(6)	1.707	2.91%
d(N1–B1) (Å)	1.501(8)	1.518	1.12%
d(Rh1–C1) (Å)	1.797(6)	1.824	1.49%

Table S3. Selected second-order interactions involving borylene boron atom in **1-BMes**.

Donor	Acceptor	$E^{(2)}$ (kcal mol^{-1})	ε_i-ε_j	$F_{i,j}$
197. LP (4) Rh	209. LP* (2) B	1.89	0.21	0.018
202. LP (1) N	209. LP* (2) B	35.17	0.30	0.093
195. LP (2) Rh	209. LP* (2) B	10.35	0.21	0.044
196. LP (3) Rh	209. LP* (2) B	6.88	0.23	0.036

Table S4. NBO-derived Wiberg Bond Indices (WBI) of selected bonds in **1-BMes** at the B3LYP/aug-cc-pVDZ level of theory.

Selected Bond	Wiberg Bond Index (WBI)
Rh1–B1	0.9308
N1–B1	0.7026
P1–N1	0.8570
P2–N2	1.0606

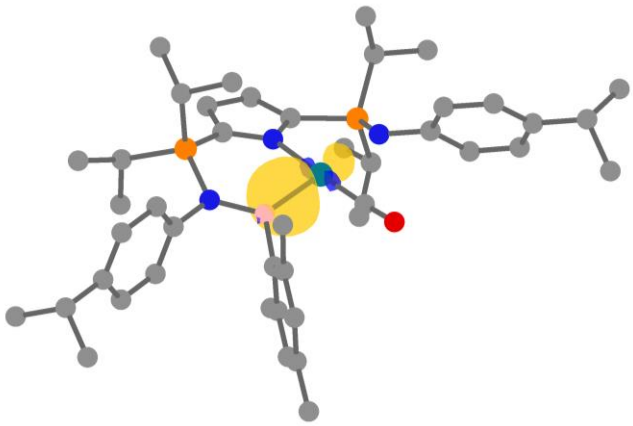

Figure S26. NBO representation of the NBO-derived Rh–B bonding orbital (occupancy: 1.807 electrons). Orbital surfaces are plotted with an isovalue of 0.08 using Gaussview. Hydrogen atoms omitted for clarity.

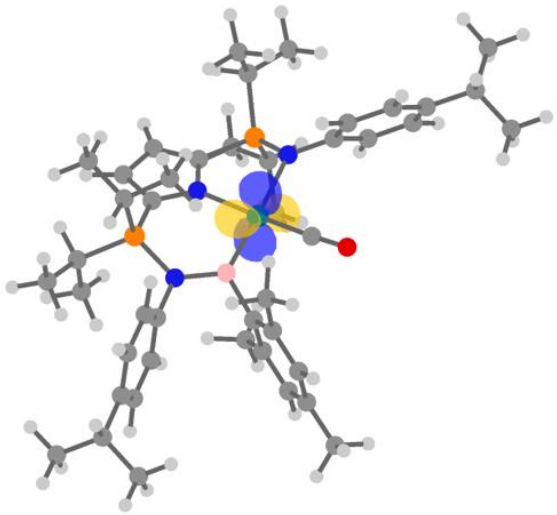

Figure S27. NBO representation of the NBO-derived Rh d_{xz} orbital (occupancy: 1.893 electrons). Orbital surfaces are plotted with an isovalue of 0.08 using Gaussview.

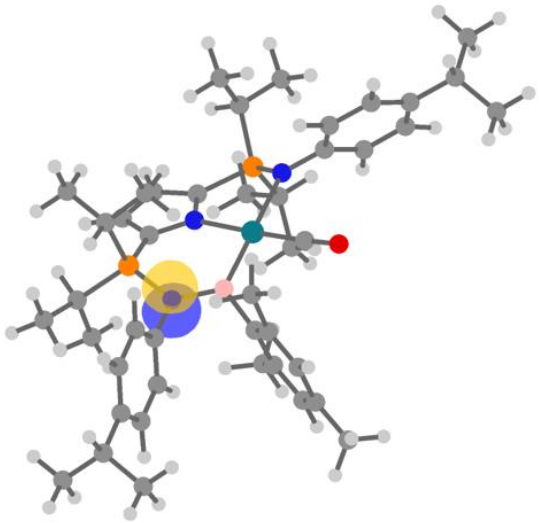

Figure S28. NBO representation of the NBO-derived N LP donor orbital (occupancy: 1.695 electrons). Orbital surfaces are plotted with an isovalue of 0.08 using Gaussview.

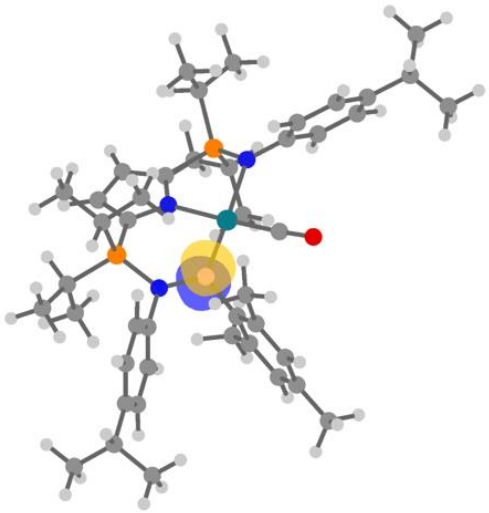

Figure S29. NBO representation of the NBO-derived B LP* acceptor orbital (occupancy: 0.271 electrons). Orbital surfaces are plotted with an isovalue of 0.08 using Gaussview.

Computational results for 1-CO·H_2BAr^F

The optimized structure of **1-CO·H_2BAr^F** was subject to NBO as well as second-order perturbation theory analysis. Notably, strong delocalization of the (B–H)σ orbital into Rh acceptor orbitals were calculated [$E^{(2)}$ = 24.9 kcal mol^{-1} and 106.5 kcal mol^{-1}].

Table S5. Comparison of DFT-calculated (B3LYP/aug-cc-pVDZ) and experimental structural parameters in **1-CO·H_2BMes**.

Parameter	Experimental	Calculated	% Difference
d(Rh1–H1) (Å)	1.61(2)	1.334	18.7%
d(P1–N1) (Å)	1.642(1)	1.676	2.05%
d(N1–B1) (Å)	1.558(2)	1.559	0.06%
d(Rh1–C1) (Å)	1.805(2)	1.822	0.94%

Table S6. Selected second-order interactions involving borylene boron atom in **1-CO·H_2BMes**.

Donor	Acceptor	$E^{(2)}$ (kcal mol^{-1})	ε_i-ε_j	$F_{i,j}$
112. BD (1) (B–H)	202. LP* Rh	106.5	0.66	0.243
112. BD (1) (B–H)	203. LP* Rh	24.9	0.67	0.125
199. LP (2) Rh	1211. BD* (B–H)	3.17	0.56	0.038
200. LP (3) Rh	1211. BD* (B–H)	2.44	0.60	0.035

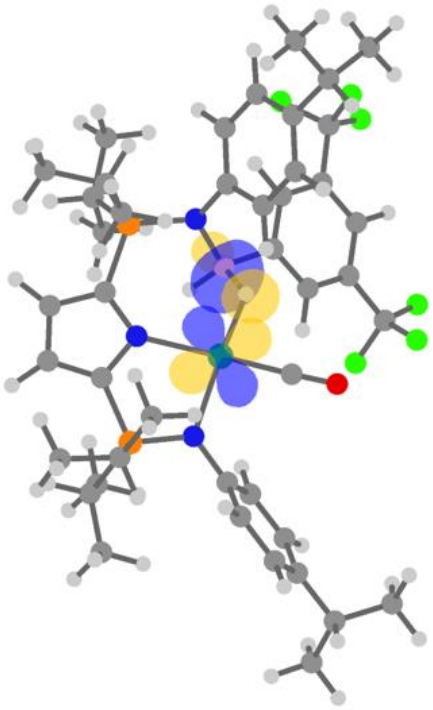

Figure S30. NBO representation of Rh $4d_{xy}$ donation to an acceptor (B–H)σ*; $E^{(2)}$ = 2.44 kcal mol^{-1}. Orbital surfaces are plotted with an isovalue of 0.08 using Gaussview.

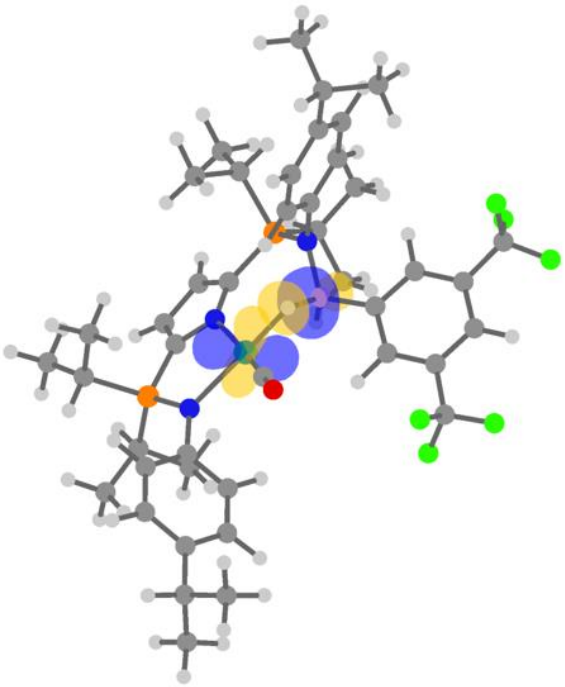

Figure S31. NBO representation of Rh $4d_{xz}$ donation to an acceptor (B–H)σ*; $E^{(2)}$ = 3.17 kcal mol^{-1}.Orbital surfaces are plotted with an isovalue of 0.08 using Gaussview.

VII. References

1. A. B. Pangborn, M. A. Giardello, R. H. Grubbs, R. K. Rosen, F. J. Timmers, *Organometallics* **1996**, *15*, 1518–1520.

2. a) S. K. Mellerup, C. Li, J. Radtke, X. Wang, Q.-S. Li, S. Wang, *Angew. Chem. Int. Ed.* **2018**, *57*, 9634–9639. b) K. Samigullin, M. Bolte, H.-W. Lerner, M. Wagner, *Organometallics* **2014**, *33*, 3564–3569.

3. C. S. MacNeil, P. G. Hayes, *Chem. Eur. J.* **2019**, *25*, 8203–8207.

4. G. R. Fulmer, A. J. M. Miller, N. H. Sherden, H. E. Gottlieb, A. Nudelman, B. M. Stoltz, J. E. Bercaw, K. I. Goldberg, *Organometallics* **2010**, *29*, 2176–2179.

5. C. P. Rosenau, B. J. Jelier, A. D. Gossert, A. Togni, *Angew. Chem. Int. Ed.* **2018**, *57*, 9528–9533.

6. J. Sandstrøm, *Dynamic NMR Spectroscopy*; Academic Press: New York, 1982.

7. G. M. Sheldrick, *Acta Crystallogr. Sect. A* **2015**, *71*, 3–8.

8. G. M. Sheldrick, *Acta Crystallogr. Sect. C* **2015**, *71*, 3–8.

9. O. V. Dolomanov, L. J. Bourhis, R. J. Gildea, J. A. K. Howard, H. Puschmann, *J. Appl. Crystallogr.* **2009**, *42*, 339–341.

10. A. Spek, *J. Appl. Crystallogr.* **2003**, *36*, 7–13.

11. Gaussian 16, Revision B.01, M. J. Frisch, G. W. Trucks, H. B. Schlegel, G. E. Scuseria, M. A. Robb, J. R. Cheeseman, G. Scalmani, V. Barone, G. A. Petersson, H. Nakatsuji, X. Li, M. Caricato, A. V. Marenich, J. Bloino, B. G. Janesko, R. Gomperts, B. Mennucci, H. P. Hratchian, J. V. Ortiz, A. F. Izmaylov, J. L. Sonnenberg, D. Williams-Young, F. Ding, F. Lipparini, F. Egidi, J. Goings, B. Peng, A. Petrone, T. Henderson, D. Ranasinghe, V. G. Zakrzewski, J. Gao, N. Rega, G. Zheng, W. Liang, M. Hada, M. Ehara, K. Toyota, R. Fukuda, J. Hasegawa, M. Ishida, T. Nakajima, Y. Honda, O. Kitao, H. Nakai, T. Vreven, K. Throssell, J. A. Montgomery, Jr., J. E. Peralta, F. Ogliaro, M. J. Bearpark, J. J. Heyd, E. N. Brothers, K. N. Kudin, V. N. Staroverov, T. A. Keith, R. Kobayashi, J. Normand, K. Raghavachari, A. P. Rendell, J. C. Burant, S. S. Iyengar, J. Tomasi, M. Cossi, J. M. Millam, M. Klene, C. Adamo, R. Cammi, J. W. Ochterski, R. L. Martin, K. Morokuma, O. Farkas, J. B. Foresman, and D. J. Fox, Gaussian, Inc., Wallingford CT, 2016.

12. A. D. Becke, *J. Chem. Phys.* **1993**, *98*, 5648–5652.

13. D. Figgen, K. A. Peterson, M. Dolg, H. Stoll, *J. Chem. Phys.* **2009**, *130*, 164108.

14. GaussView, version 5.0 Gaussian, Inc., Wallingford, CT, **2016**.

15. NBO, version 6.0. E. D. Glendening, J. K. Badenhoop, A. E. Reed, J. E. Carpenter, J. A. Bohmann, C. M. Morales, C. R. Landis, F. Weinhold, Theoretical Chemistry Institute, University of Wisconsin, Madison, **2013**.

16. J. P. Foster, F. Weinhold, *J. Am. Chem. Soc.* **1980**, *102*, 7211–7218.